ISSN 2095-6037
CN 11-2277/P

# JMR Journal of Meteorological Research

Volume 31 Number 4 August 2017

气 象 学 报


Chinese Meteorological Society

Springer

VOLUME 31 JOURNAL OF METEOROLOGICAL RESEARCH AUGUST 2017

# An Overview of Mineral Dust Modeling over East Asia

Siyu CHEN[1], Jianping HUANG[1*], Yun QIAN[2], Chun ZHAO[2], Litai KANG[1], Ben YANG[3], Yong WANG[4], Yuzhi LIU[1], Tiangang YUAN[1], Tianhe WANG[1], Xiaojun MA[1], and Guolong ZHANG[1]

1 *Key Laboratory for Semi-Arid Climate Change of the Ministry of Education*, *Lanzhou University*, *Lanzhou* 730000, *China*
2 *Atmospheric Science and Global Change Division*, *Pacific Northwest National Laboratory*, *Richland*, *WA* 99354, *USA*
3 *School of Atmospheric Sciences*, *Nanjing University*, *Nanjing* 210089, *China*
4 *Department of Earth System Science*, *Tsinghua University*, *Beijing* 100084, *China*

(Received August 21, 2016; in final form January 20, 2017)

ABSTRACT

East Asian dust (EAD) exerts considerable impacts on the energy balance and climate/climate change of the earth system through its influence on solar and terrestrial radiation, cloud properties, and precipitation efficiency. Providing an accurate description of the life cycle and climate effects of EAD is therefore critical to better understanding of climate change and socioeconomic development in East Asia and even worldwide. Dust modeling has undergone substantial development since the late 1990s, associated with improved understanding of the role of EAD in the earth system. Here, we review the achievements and progress made in recent decades in terms of dust modeling research, including dust emissions, long-range transport, radiative forcing (RF), and climate effects of dust particles over East Asia. Numerous efforts in dust/EAD modeling have been directed towards furnishing more sophisticated physical and chemical processes into the models on higher spatial resolutions. Meanwhile, more systematic observations and more advanced retrieval methods for instruments that address EAD related science issues have made it possible to evaluate model results and quantify the role of EAD in the earth system, and to further reduce the uncertainties in EAD simulations. Though much progress has been made, large discrepancies and knowledge gaps still exist among EAD simulations. The deficiencies and limitations that pertain to the performance of the EAD simulations referred to in the present study are also discussed.

**Key words:** East Asia, dust aerosol, dust modeling, dust emissions, long-range dust transport, dust radiative forcing

**Citation:** Chen, S. Y., J. P. Huang, Y. Qian, et al., 2017: An overview of mineral dust modeling over East Asia. *J. Meteor. Res.*, **31**(4), 633–653, doi: 10.1007/s13351-017-6142-2.

## 1. Introduction

Dust, one of the major aerosol species contributing to global aerosol burden and optical depth, is a highly active component of the physical, chemical, and biogeochemical cycles of the earth system (Qian et al., 1999). As the second largest contributor of dust aerosols in the world, approximately 2000 Mt of desert dust from East Asia is injected into the atmosphere annually. Of this amount, approximately 30% is re-deposited onto the region's deserts, 20% is transported at the regional scale primarily within continental China, and the remaining 50% is transported farther eastwards to Korea, Japan, the Pacific islands, and across the Pacific Ocean to the United States, Canada, and even Greenland (e.g., Zhang et al., 1997; Liao and Seinfeld, 1998; Qian et al., 1999; Gong et al., 2003b, 2006; Huang et al., 2008a, 2012, 2016; Uno et al., 2008; Wang et al., 2008; Eguchi et al., 2009; Fu et al., 2009; Liao et al., 2009; Shao et al., 2011; Li et al., 2011, 2012; Wang S. H. et al., 2012; Kang et al., 2016).

Such a large amount of East Asian dust (EAD) has a considerable impact on the regional climate by altering the radiative balance between incoming solar and outgo-

Supported by the National Natural Science Foundation of China (41405003 and 41521004). Authors Yun Qian and Chun Zhao were supported by the Office of Science, U.S. Department of Energy (DOE), as part of its Regional and Global Climate Modeling Program. The Pacific Northwest National Laboratory is operated for the DOE by the Battelle Memorial Institute under contract DE-AC05-76RL01830.

*Corresponding author: hjp@lzu.edu.cn.

ing terrestrial radiation in the atmosphere (the "direct effect") (Han et al., 2004, 2012; Su et al., 2008; Huang et al., 2009; Han, 2010; Bi et al., 2011; Wang J. et al., 2012; Wang Z. L. et al., 2013). Moreover, EAD can modify the microphysical properties of clouds and the precipitation efficiency in the earth system (the "indirect effect" or "semi-direct effect") (Yin et al., 2002; Wang H. et al., 2004; Huang et al., 2006a, b, 2010, 2014; Yin and Chen, 2007; Su et al., 2008; Qian et al., 2009; Chen et al., 2010; Jia et al., 2010; Guo and Yin, 2015). Dust particles also provide key mineral supplement to influence oceanic $CO_2$ uptake and nutrients in the ocean and rain forest via long-distance transport, and then modulate the ecosystem and carbon cycle at both regional and global scales (Shao et al., 2011). In addition, EAD induces highly adverse effects on social and economic development. For example, a severe dust storm in South Korea caused enormous economic loss and human suffering, costing approximately US $5600 million (0.8% of GDP). The total economic loss due to dust storms in Beijing ranged from 2268.5 million RMB (US $273.3 million) to 5796 million RMB (US $698.3 million), according to Ai and Polenske (2008). Increased concentrations of particulate matter in the atmosphere during dust storms can also lead to acute damage to respiratory systems and long-term damage such as desert pneumoconiosis (Kang et al., 2013; Kameda et al., 2016).

The development of dust modeling has greatly improved the comprehension of dust-related processes and the effects of dust on the environment and climate over the last 30 years. Early studies of dust modeling were conducted by Westphal et al. (1988) and Joussaume (1990). Studies of dust models at the global scale include those by Tegen and Fung (1994), Woodward (2001), Zender et al. (2003), and Huneeus et al. (2011). Studies of dust models at the regional scale include those by Shao et al. (1996), Marticorena et al. (1997), Wang et al. (2000), Uno et al. (2003), Han et al. (2004, 2012), Han (2010), and Wang H. et al. (2010). Compared with studies of dust simulations in other regions, the estimation of EAD is more challenging because of the complex meteorological conditions, topography, and land use in East Asia. Nevertheless, important progress in EAD simulations has been made in recent decades. More advanced EAD modeling has been conducted by CEMSYS (Shao et al., 1996; Shao, 2001), IAPS (Sun et al., 2012), ITR (Tegen et al., 1996), CFORS (Uno et al., 2009), COAMPS (Liu et al., 2003), ADAM (In and Park, 2003), MASINGAR (Tanaka and Chiba, 2005), NARCM (Gong et al., 2003a), CUACE/dust (Zhou et al., 2008), WRF-Chem/dust (Zhao et al., 2010, 2011, 2013a, b; Chen et al., 2013, 2014a), WRF-dust (Bian et al., 2011), RegCM4/dust (Sun et al., 2012), and CMAQ/dust (Fu et al., 2014), among others. Such modeling has produced valuable information at the mechanistic level, shedding light on EAD phenomena and their detailed physical processes. Nevertheless, significant discrepancies among numerical models have been documented regarding the physical and chemical properties of dust, and in representations of dust's radiative effects (e.g., Shao et al., 2003; Uno et al., 2006; Ma et al., 2007; Yumimoto et al., 2008; Huneeus et al., 2011; Huang et al., 2014; Liu et al., 2014).

This paper provides a review of the modeling framework for EAD-related physical processes and the associated radiative forcing (RF) and climate effects. A state-of-the-art model, the Weather Research and Forecasting model with Chemistry (WRF-Chem), is used to show the regional and seasonal variations of dust mass loading and its radiative effect over East Asia. Section 2 describes recent achievements in estimating dust emissions over East Asia. Section 3 summarizes the modeling of the long-range transport of EAD. Section 4 discusses the climate effects of EAD. Finally, several issues related to the achievements, uncertainties, and challenges involved in dust modeling are discussed in Section 5.

## 2. Dust emissions

### 2.1 *Dust emission schemes*

Dust particles can be dispersed by turbulence into the free atmosphere, transported to remote regions by winds, and eventually deposited back onto the earth's surface. Dust emissions are also a key component of the dust cycle, which greatly influences other dust-related processes such as the energy and carbon cycle at the global scale in the earth system (Shao et al., 2011). Han et al. (2004), Zender et al. (2003), Shao and Dong (2006), and Shao et al. (2011) classified dust-emission schemes into three categories. In this paper, we focus on two major dust emission schemes in EAD simulations, hereafter referred to as Scheme I and Scheme II.

(1) Scheme I: The dust emission flux is a function of wind speed or friction speed with an empirical size distribution upon the emitted dust. This scheme was used by Tegen and Fung (1994), Mahowald et al. (1999), Ginoux et al. (2001), Perlwitz et al. (2001), Zender et al. (2003), and Bian et al. (2011). Here, we use the Georgia Tech/Goddard Global Ozone Chemistry Aerosol Radiation and Transport (GOCART) dust scheme (Ginoux et al., 2001) to illustrate this approach. The entire bare ground surface is assumed as a potential dust source in this scheme. The dust emission flux is expressed as a

function of the surface wind speed and soil wetness. The GOCART scheme calculates the dust emission flux $G$ (μg m$^{-2}$ s$^{-1}$) as

$$G = C\,S\,s_p\,u_{10\mathrm{m}}^2(u_{10\mathrm{m}} - u_t), \tag{1}$$

where $C$ (μg s$^2$ m$^{-5}$) is an empirical proportionality constant (the default value of $C$ is set to 1 μg s$^2$ m$^{-5}$); $S$ is a semi-empirical dust source function that defines potential dust source regions based on underlying surface factors such as the vegetation and snow cover; $s_p$ is the fraction of emissions for each dust-size class; $u_{10\mathrm{m}}$ is the horizontal wind speed at 10-m height; and $u_t$ is the threshold wind velocity for triggering dust emissions, which is a function of the particle size, air density, and surface soil moisture. Notably, the value of the empirical proportionality constant $C$ is highly tunable because it depends on regionally specific data. Generally, we tune $C$ to keep the modeled aerosol optical depth (AOD) consistent with the observational data, such as AERONET measurements or Multi-angle Imaging Spectroradiometer (MISR) and Moderate Resolution Imaging Spectroradiometer (MODIS) retrievals (Zhao et al., 2010, 2011; Chen et al., 2013, 2014a).

(2) Scheme II: This scheme is physically explicit and more complex. It uses sophisticated mechanisms of dust production to predict the size-resolved dust emissions (Shao, 2001, 2004, 2008; Kok, 2011). Shao (2008) divided this dust emission scheme into three parts: saltation bombardment, aggregate disintegration, and aerodynamic entrainment. In recent years, dust emission schemes have included one or both of the first two mechanisms (Lu and Shao, 1999; Shao, 2004) because these two mechanisms are efficient and the most important (Klose et al., 2014). The dust emission scheme of Shao (2004) is calculated as follows:

$$\tilde{F}(d_i, d_s) = c_y \eta_{fi} [(1-\gamma) + \gamma\alpha_p](1+\alpha_m)\frac{gQ}{u_*^2}, \tag{2}$$

$$\alpha_m = 12u_*^2\frac{\rho_b}{P}\left(1 + 14u_*\sqrt{\frac{\rho_b}{P}}\right), \tag{3}$$

$$\gamma = \exp\left[-(u_* - u_{*t})^3\right], \tag{4}$$

where $\tilde{F}$ is the dust emission flux (μg m$^{-2}$ s$^{-1}$) for the particle group of size $d_i$, generated by the saltation of particles of size $d_s$; $c_y$ is a dimensionless coefficient; $\eta_{fi}$ is the total dust fraction; $\gamma$ is a weighting function; $Q$ is the streamwise saltation flux of $d_s$; $g$ is acceleration due to gravity; $u_*$ is the friction velocity; $\alpha_m$ is the ratio of the mass of the impacting particle to the mass ejected by bombardment; $\rho_b$ is the ratio of free dust to aggregated dust; and $P$ is the soil plastic pressure.

The dust emission from bin $i$ is given by

$$\tilde{F}(d_i) = \int_{d_1}^{d_2} \tilde{F}(d_i, d)\,P(d)\,\delta d, \tag{5}$$

where $d_1$ and $d_2$ define the lower and upper size limit, respectively, for saltating particles.

The total dust emission rate is estimated as follows:

$$F = \sum_{i=1}^{I} \tilde{F}(d_i). \tag{6}$$

Aerodynamic dust entrainment has not been included in traditional dust emission schemes because the intensity of aerodynamic dust emissions is much weaker than that of strong dust storms. However, this process may occur frequently, which may be a major contributor to regional or global dust budgets. Klose and Shao (2012) proposed the first comprehensive CTDE (Convective Turbulent Dust Emission) model and further estimated the contribution of convective dust emissions to the regional/global dust budget. Klose and Shao (2013) developed a large-eddy dust model (WRF-LES/D) with this new CTDE scheme to investigate the CTDE processes for various conditions of boundary-layer stability and wind fields for a given soil type. Based on Klose and Shao (2012, 2013), Klose et al. (2014) developed an improved parameterization scheme for CTDE, which provides a new description of instantaneous momentum flux and a correction function for the cohesive force to consider the effect of soil moisture, and the lifting force to consider the effect of vegetation roughness. The dust emission flux is given as

$$\tilde{F} = \frac{\alpha_N}{2D}\left\{-w_t m_p + T_p\left(f - f_i\frac{d}{D}\right)\right\}, \quad \text{for } f > f_t, \tag{7}$$

where $D$ is the viscous sub-layer thickness, $w_t$ is the particle terminal velocity, $m_p$ is the particle mass, $T_p$ is the particle response time, $f$ is a given lifting force, $f_i$ is the cohesive force, and $d$ is the particle diameter. As shown in Klose and Shao (2012), $\alpha_N = N_p D$, $N_p$ is the particle number concentration. Thus, $\alpha_N$ has the dimensions of [m$^{-2}$] and can be interpreted as the over $D$ integrated particle number concentration per unit area. Accordingly, $\alpha_N$ decreases with particle size as follows:

$$\alpha_N = \alpha_{N_0}\left(\frac{d}{d_{\mathrm{ref}}}\right)^{-3}, \tag{8}$$

where $\alpha_{N_0}$ is an empirical constant of dimensions [m$^{-2}$] and $d_{\mathrm{ref}}$ is the particle size for which the scheme is calibrated.

CTDE is initiated only if $f$ exceeds the retarding force $f_t = f_i + m_\rho g$, where $g$ is the gravitational acceleration. For given distribution functions for the lifting force $p(f)$ and inter-particle cohesive force $p_j(f_i)$ corresponding to particle size $d_j$, the dust emission flux can be obtained as follows:

$$F_j = \int_0^\infty [\int_0^f \tilde{F} \cdot p_j(f_i)\, \mathrm{d}f_i]\, p(f)\, \mathrm{d}f, \tag{9}$$

where $F_j$ represents the dust emissions from bin $j$, $p_j(f_i)$ is the PDF of $f_i(d_j)$, and $p(f)$ is the PDF of $f$. The total dust emission flux is

$$F = \int_0^{d_{\max}} F_j \cdot P_A(d_j)\, \delta d_j, \tag{10}$$

where $d_{\max}$ is the maximum dust particle diameter (20 μm in this study), and $P_A(d_j)$ is the area's particle size distribution (PSD). Note that $P_A$ is used instead of mass PSD, $P_M$, because the surface shear stress acts on the particle area instead of the particle volume. The $P_M(d_j)$ is usually directly available from particle size analysis, but for a given $P_M$, $P_A$ can be estimated as

$$P_A(d_j) = \frac{P_M(d_j)}{d_j}\left[\sum_{k=1}^{N} \frac{P_M(d_k)\,\delta d_k}{d_k}\right]^{-1}. \tag{11}$$

### 2.2 *Simulation of dust emissions*

Dust simulation research has shown that modeled vertically integrated parameters (e.g., AOD) are reproduced within a factor of 2 or 3, whereas the dust emissions are reproduced within a factor of 10, on the global scale (Zender et al., 2003; Todd et al., 2008; Huneeus et al., 2011). Quantification of dust emissions over East Asia is hampered by the uncertainties of dust production mechanisms, complex local geomorphological and topographical features, and various parameters of surface properties (e.g., soil composition, soil texture, soil wetness, vegetation, and land use) (Chao and Alexander, 1984; Zhao et al., 2006; Yumimoto et al., 2008; Bian et al., 2011).

To better understand and demonstrate dust emission properties over East Asia, a number of large field campaigns [e.g., APEX (Asian Atmospheric Particulate Environmental Change Studies), ACE-Asia (Asian Pacific Regional Aerosol Characterization Experiment), and ADEC (Aeolian Dust Experiment on Climate Impact) (Takemura et al., 2003; Mikami et al., 2006; Uno et al., 2006; Huang et al., 2008b, 2011; Ge et al., 2011; Chen et al., 2013, 2014b; Zhao et al., 2013b), together with advanced retrieval methods for remote sensing (Wang and Min, 2008; Wang and Huang, 2009) that address EAD related problems, have been conducted over the last few decades, providing a benchmark test dataset for the development of EAD parameterization schemes in numerical models. Gong et al. (2003a) incorporated a detailed soil texture map and an up-to-date distribution of desertification in China in the dust emission scheme. The observed soil grain-size distribution, water moisture, and meteorology could be used to optimize the appropriate parameters and conditions for Chinese soil dust emissions and transport. The simulated dust concentrations in source regions and areas downwind of eastern China to North America compare well with ground-based and aircraft measurements, as well as satellite retrievals, in East Asia and North America (Gong et al., 2003a; Zhao et al., 2003). Chen et al. (2014a) used the GOCART dust emission scheme coupled with the WRF-Chem model to evaluate and compare with observed EAD in 2007–11. A comparison of MISR retrievals and WRF-Chem model simulations over the Taklimakan Desert (TD) and Gobi Desert (GD) in 2007–11 is shown in Fig. 1. The results indicate that the GOCART dust emission scheme adequately captures the monthly variations of dust AOD in the dust source regions.

However, the uncertainty in the simulated EAD emission flux is still severe in numerical models. Uno et al. (2006) compared eight dust models coupled with eight dust emission schemes over East Asia in an intercomparison study. They noted that numerical modeling correctly predicted the onset and ending of EAD events, but large differences with respect to dust emissions were apparent. The wide range of estimated dust emission fluxes over East Asia may be partly due to the differences in dust emission schemes among these simulations, but we cannot ignore the difference in other respects, such as meteorological conditions, dust size parameterization, and land-cover data used. Therefore, Kang et al. (2013) performed a parallel comparison among three dust emission schemes [Marticorena and Bergametti, 1995, Lu and Shao, 1999 (saltating bombardment only), and Shao, 2004 (both saltating bombardment and aggregate disintegration)—hereinafter referred to as MB, LS, and S04, respectively] with the same WRF-Chem model configuration. The large differences in vertical dust fluxes among different emission schemes ranged from a factor of approximately 100 for clay to 10 for sand.

Overall, the uncertainties in dust emissions over East Asia derive mainly from the following two causes:

(1) Dust emission mechanism. Dust from soil grains

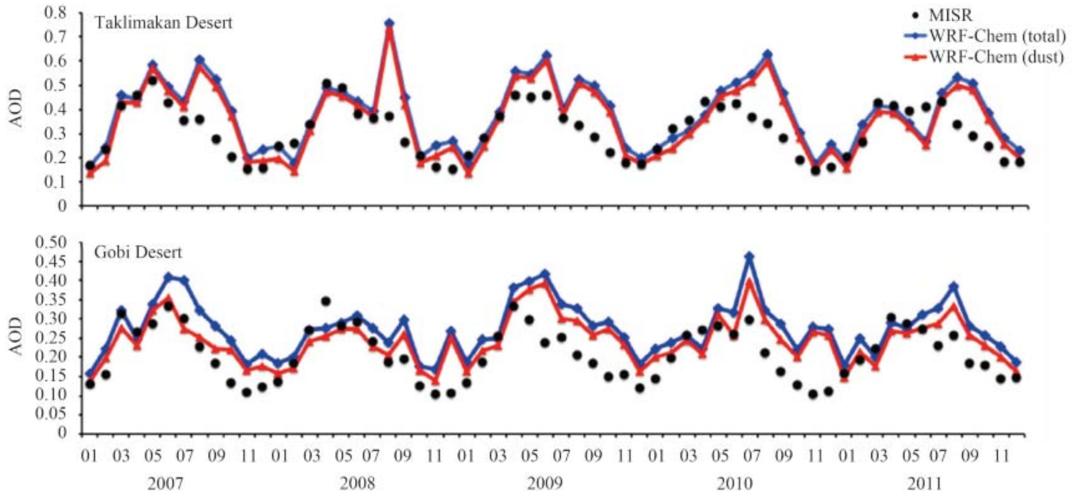


**Fig. 1.** Monthly total AOD over the Taklimakan Desert and Gobi Desert from MISR retrievals (black dots) and WRF-Chem simulations (solid lines) for 2007–11. Both the total AOD (blue line) and dust AOD (red line) from the simulations are also shown (from Chen et al., 2014a).

produced by wind erosion involves complex nonlinear processes governed by meteorology. Scheme I is relatively simple and easier to apply in practice. The drawback is its empirical or semi-empirical nature, which lacks a physical mechanism for dust emissions. Scheme II considers sophisticated wind-erosion physics and dust emission mechanisms, which are more accurate and complex than Scheme I. This scheme improves in understanding of the dust emission mechanism and enhances the accuracy of dust emission prediction. However, a large number of input parameters that are difficult to estimate in Scheme II also add to the uncertainties in the simulated dust emission fluxes. For the LS and SO4 schemes, the dust emission flux is most sensitive to the plastic pressure. The appropriate tuning of parameters in Scheme II becomes important in dust modeling.

(2) Soil/surface information. The spatial distributions of land-surface properties over East Asia strongly affect the intensity of EAD emissions. Uno et al. (2006) argued that accurate soil/surface conditions and land surface information are more important than the complexity of the dust emission scheme. Therefore, the lack of detail with respect to land surface conditions (e.g., soil texture, surface roughness length, moisture content, soil particle size distribution, vegetation cover, land cover type, and snow cover), and the dearth of observations over the dust source regions of East Asia, have been a major obstacle to reducing the uncertainties in simulating dust emission fluxes (Sokolik and Golitsyn, 1993; Gong et al., 2003b; Zhao et al., 2006). Moreover, different size distributions of emitted dust may also add uncertainties in dust simulation (Zhao et al., 2013a).

## 3. Dust transport

Dust particles, along their long-range transport, can significantly change RF, atmospheric chemistry, and biogeochemical cycles of the atmosphere, land, and ocean, even into remote regions (Wang et al., 2000, 2004; Wang X. et al., 2010; Liu et al., 2011, 2010). Despite its climatic and geochemical importance, dust transport, based on both ground-based and satellite observations, is difficult to be captured sufficiently because it ranges from short durations at the regional scale to long durations at the global scale. Numerical modeling provides an alternative and systematic approach for investigating horizontal and vertical distributions as well as the seasonal and interannual variability of EAD in long-range transport.

### 3.1 *Eastward and southeastward transport*

The eastward/southeastward transport of EAD exerts significant impacts on the environment, human health, and climate/climate change over East Asia, given EAD's high association to anthropogenic emissions (Huang et al., 2006c; Li et al., 2011; Han et al., 2012; Wang J. et al., 2012; Hsu et al., 2013). The long-distance transport of EAD supplies mineral elements to the northern South China Sea, and thus remarkably enhances phytoplankton growth by enriching the chlorophyll-a concentration (Wang S. H. et al., 2012). In addition, EAD is also adsorbed by nitric acid, suppressing the cycle of nitrogen oxides and decreasing the Asian pollution effect on surface ozone in America (Fairlie et al., 2010). Moreover, EAD also has important implications for atmospheric pollution, since the acidic surface of dust can accelerate the nitration reactions of polycyclic aromatic hydrocarbons (PAHs) in the atmosphere, and thus the nitrated polycyclic aromatic hydrocarbons (NPAHs) increase dramatically during dust storms. NPAHs can enhance the toxicity of EAD in urban environments, which has adverse effects on people's health, e.g., through carcinogenicity (Kameda et al., 2016).

Dust storms over East Asia occur mainly in spring, due to the considerable instability of synoptic weather systems during this season. Results show that cold-air outbreaks induced by Mongolian cyclonic and frontal systems lead to about 78% of all dust storms in China (Sun et al., 2001; Huang et al., 2008b). Dust particles can be uplifted to high levels by upward motion and turbulent mixing, and are then transported farther to Korea, Japan, and across the Pacific Ocean to the United States by westerly winds (Gong et al., 2003a; Huang et al., 2012; Wang J. et al., 2012; Chen et al., 2016). The pathways of cold-air outbreaks can be divided into three broad categories: north (32%), northwest (41%), and west (27%). Evidently, the northwest route is the predominant one (Sun et al., 2001).

In particular, a strong dust storm originating from the GD moved eastwards, southeastwards, and southwards, successively, in March 2010, even reaching and attacking the Pearl River Delta (such as Hong Kong) and the South China Sea (Li et al., 2011; Wang S. H. et al., 2012), which was a unique case compared with previous ones that mostly moved eastwards. This southward-moving dust storm attracts considerable interest from researchers, yielding many studies on its environment and climatic effects. According to Li et al. (2011), it was the special synoptic conditions, i.e., the high pressure at the surface shifting to the Yellow Sea and then mixing with low pressure at the surface, inducing northerly and northeasterly winds, thus resulting in dust particles being transported back to the continent from the sea and influencing the Pearl River Delta, which was unique compared with the dust storms in March 2002 and 2006. This southeastward transport of EAD was extremely severest and the $PM_{10}$ concentration was above 400 mg m$^{-3}$ over western China and the GD, and below 100 mg m$^{-3}$ in remote regions such as Japan. Besides, dust aerosol was a main contributor to the $PM_{10}$ concentration. Furthermore, dust deposition during the dust storm of March 2010 was disproportionate. The relatively finer size of dust particles with a low dry deposition ratio led to the increase in dust concentration. The dry deposition velocities at peak time were about 0.2–0.6 cm s$^{-1}$, far lower than usual (1–2 cm s$^{-1}$), which indicates that, in some cases, the synoptic conditions of the atmosphere can be more important than the strength of the dust storm, in terms of the southeastward transport of EAD to the South China Sea (Hsu et al., 2013). In addition, Chen et al. (2016) also noted that the GD was located in the warm zone before the approach of a cold front from the northwest, where enhanced convection increased the momentum transfer in the middle and lower troposphere. Moreover, the GD is located in a relatively flat, high-altitude region influenced by the confluence of the northern and southern westerly jets. Therefore, GD dust transmission was the ubiquitous contribution over East Asia. Compared with the quantity of the TD dust contribution to the dust sink in March 2010 (1.1 ton day$^{-1}$), that of the GD dust was significantly greater (1.4 ton day$^{-1}$).

The vertical distribution of dust aerosols during transport is crucial for estimating dust radiative heating rates (Sokolik and Golitsyn, 1993; Sokolik and Toon, 1996; Kim et al., 2006, 2011). However, the vertical distribution of dust is difficult to measure. The development of lidar and passive infrared remote sensors, e.g., IASI (the Infrared Atmospheric Sounding Interferometer) and AIRS (Atmospheric Infrared Sounder), have facilitated the detection of dust vertical structure. In particular, the Cloud–Aerosol Lidar and Infrared Pathfinder Satellite Observations (CALIPSO) satellite, which was launched in April 2006 and has two-wavelength depolarization lidar CALIOP devices on board, enable the accurate determination of the three-dimensional (3D) transport of aerosols at the global scale, especially for aerosol vertical distributions (Huang et al., 2008b; Liu et al., 2008).

Many studies have attempted to describe the spatial distribution and vertical structure of EAD by combining dust modeling with satellite/ground-based lidar observations, which provides comprehensive and reliable analyses of the 3D structure of EAD and sheds new insights into long-term EAD transport. These combinations can not only overcome the observational shortcomings such as the limited spatial and temporal coverage, but also help dig out the mechanisms involved in the long-range transport of EAD. Uno et al. (2009) used the SPRINTARS model and CALIOP retrievals to investigate the transport of dust clouds generated in the TD. The simulated dust extinction coefficients agreed well with the CALIOP retrievals in the transport pathway. Yumimoto et al. (2009, 2010) and Eguchi et al. (2009) also reproduced the 3D structure of intercontinental dust transport from the TD to the Pacific Ocean, North America, and the Atlantic Ocean, using similar tools. Furthermore, studies have focused on EAD transport by using a

4DVar (four-dimensional variational) data assimilation system of regional dust modeling (RAMS/CFORS-4DVar) (Yumimoto et al., 2008, 2009). Compared with 3DVar, 4DVar could simultaneously add to the temporal variations of lidar observations. The vertical distribution of simulated dust extinction coefficients was comparable to that from the CALIPSO results. An increase in EAD emissions (approximately 31%) in the data assimilation was observed, especially over the Mongolian region (Uno et al., 2008; Yumimoto et al., 2008).

### 3.2 *Southward transport*

As discussed above, the eastward transport of EAD is common and has been elaborated on by many studies. Huang et al. (2007) firstly observed the southward transport of TD dust to the northern slopes of the Tibetan Plateau (TP) during summer based on CALIOP retrievals (Fig. 2). Figure 2 shows the dust layer that appeared along the northern slopes of the TP and extended from a height of 5–9 km above mean sea level. This study enhances our knowledge of EAD transport and furthers our understanding of the impact of the TP with transported dust aloft on regional and global climates. Xia et al. (2008) pointed out that, compared with springtime, the correlation of the seasonal variation of the AOD over the TP and those over the TD was closer in summertime, based on MISR retrievals. Jia et al. (2015) also found that meteorological conditions and topography benefit the transport of dust emitted adjacent to the TP towards the plateau in summer. Liu et al. (2015) further investigated the transport of summer dust and anthropogenic aerosols over the TP by implementing the SPRINTARS model with a nonhydrostatic regional model.

The mechanism of this observed southward transport of the TD dust in summer was investigated with the WRF-Chem model by Chen et al. (2013). Figure 3 shows a schematic representation of the streamlines and $PM_{2.5}$ dust dry mass concentrations during 26–29 July 2006, to indicate the flow trajectories along the mountainous terrain. The dust originated from the TD and propagated towards the TP under the steering of easterly winds. The flow trajectories were close to the ground on 26–27 July (Figs. 3a, b), but were no longer close to the ground after this date, with weakened dust emissions and increased southward transport of dust over the following days (Figs. 3c, d). A schematic representation of the emission and transport processes of TD dust near the TP is also shown. Specifically, the strong dust storm over the TD was generated by a mesoscale cold front system. Subsequently, large amounts of dust particles along the Kunlun Mountains were lifted above the northern slopes of the TP due to topographic lift and horizontal shear. The movement and development of the TP's low vortex led to strong vertical motion over the TP, resulting from the impact of the thermal effects of the TP (i.e., acting as a "heat pump"). Therefore, dust particles were lifted to the upper troposphere and formed a thick dust layer approximately 6–8 km above mean sea level, caused by strong thermal mixing. Figure 4 shows the contributions of dust emissions, transport, and dry/wet deposition to the dust mass balance in 7 regions over East Asia in 2007–11 as simulated by the WRF-Chem. The positive (negative) sign represents an increase (a decrease) in the dust concentration. The percentage is the contribution to the dust

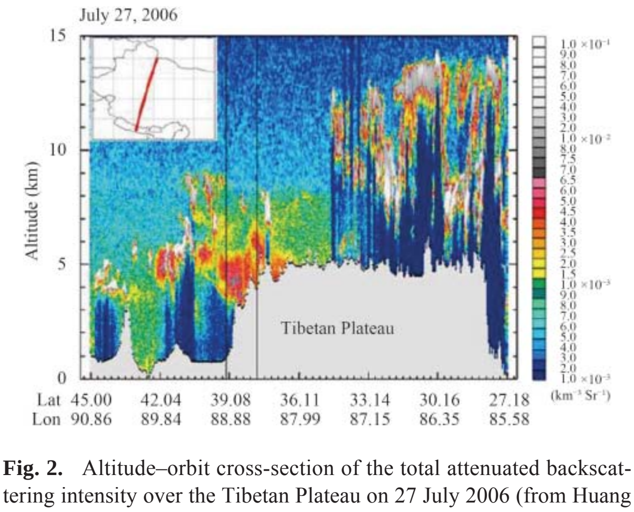


**Fig. 2.** Altitude–orbit cross-section of the total attenuated backscattering intensity over the Tibetan Plateau on 27 July 2006 (from Huang et al., 2007).

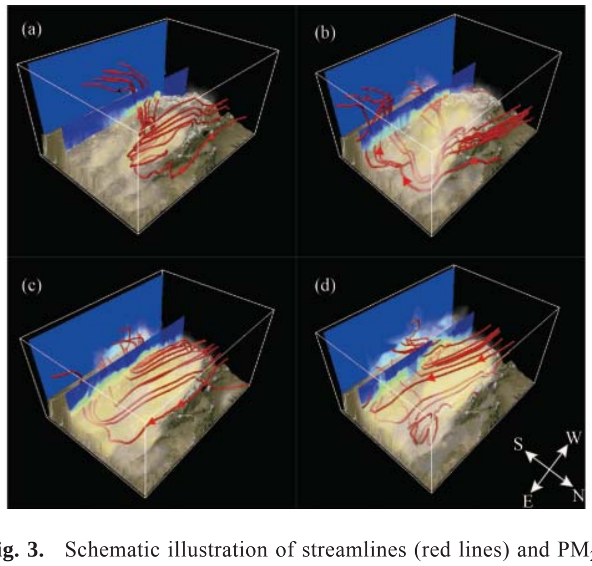


**Fig. 3.** Schematic illustration of streamlines (red lines) and $PM_{2.5}$ dust aerosol dry mass concentrations (yellow shadings) at 1200 UTC (a) 26, (b) 27, (c) 28, and (d) 29 July 2006, simulated by WRF-Chem. The 3-D streamlines also depict the direction of wind shear. The red arrows denote the direction of dust transport.

mass balance in the region. Among the four budget terms, the emission contribution is absolute positive. Overall, the contribution from dust transport (~80%) to the TP dust concentration was much larger than that from dust emissions (~20%), especially during summer and autumn (Fig. 4). Dry deposition (–51%) and wet deposition (–49%) were comparable sinks of dust in the atmosphere over the TP. TP dust could produce a net warming effect with a domain average of +0.4 W $m^{-2}$ and a maximum of +2.2 W $m^{-2}$. Dust resulted in a slight cooling effect (–0.7 W $m^{-2}$) at the surface. It could modify the atmospheric heating profile over the TP and further affect the atmospheric circulation and energy budget at both regional and global scales (Chen et al., 2013).

### 3.3 *Contributions from TD and GD dust*

Over the East Asian region, TD and GD are the major dust source regions, from which dust particles are transported eastwards to eastern and southern China, Korea, Japan, and parts of the Pacific Ocean (Huang et al., 2010; Uno et al., 2011; Huang et al., 2013). However, relative importance of the TD and GD to EAD remains unclear, with an ongoing debate as to whether the TD is the foremost source of dust over East Asia (Zhang et al., 2003; Zhang L. et al., 2010). Using observations to distinguish the contributions from TD and GD to the dust concentration over East Asia is difficult. Numerical models can be used to effectively investigate the emission, long-term transport, and wet/dry deposition of TD and GD dust (Chen et al., 2016, 2017 ). Dust emission (+100%) is the only factor contributing positively to the dust mass balance over the TD and GD, while dust transport, as well as dry and wet deposition, are sinks of dust in the atmosphere. Specifically, GD dust has a larger influence on the dust mass loading than TD dust at the regional scale. The contribution of dust transport over the GD (–36%) is larger than that over the TD (–26%). The contributions of dry and wet deposition over the GD (–42% and –22%, respectively) are less than those over the TD (–49% and –25%, respectively) (Fig. 4). The tendency of GD dust transport is approximately –24.8 g $m^{-2}$ each season, which is 35.1% of GD dust emission during the spring (Chen et al., 2016).

The differences in the topography, elevation, and dynamic and thermodynamic environmental conditions of the TD and GD lead to differences in the dust emission, lifting height of dust, and long-distance transport of dust. The GD is located at a confluence of the southern and northern branches of the upper-level jet stream. The downward momentum transport produced by a high-

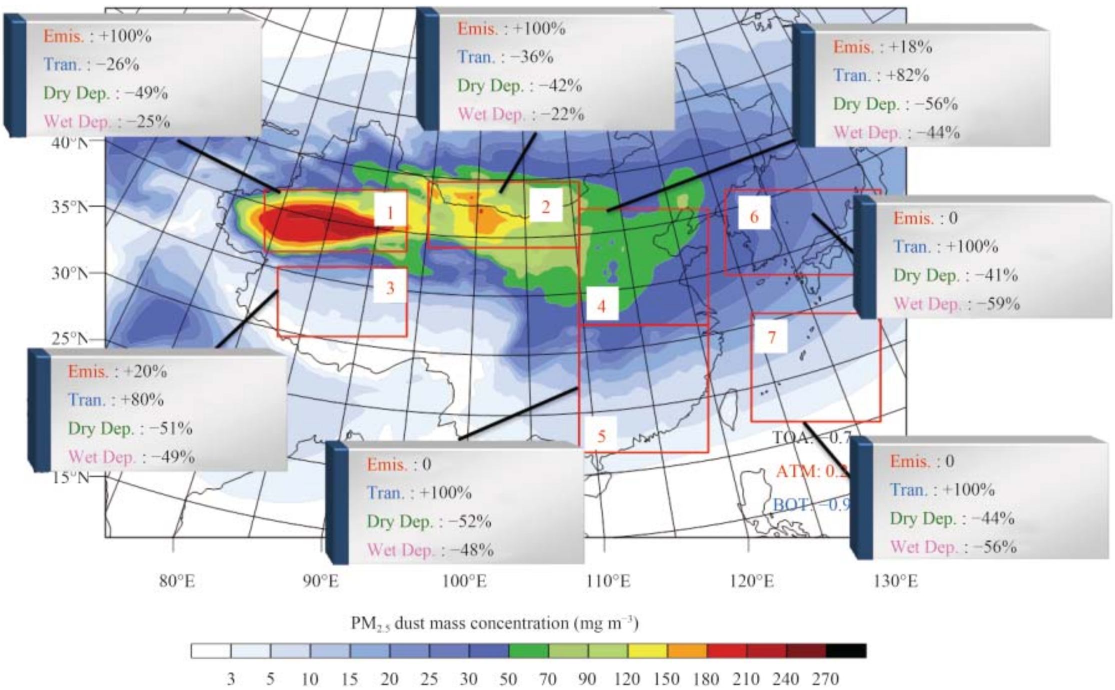


**Fig. 4.** Spatial distribution of the $PM_{2.5}$ dust mass concentration (mg $m^{-3}$) for 2007–11 over East Asia from WRF-Chem simulations. Seven regions [1: Taklimakan Desert (TD); 2: Gobi Desert (GD); 3: Tibetan Plateau (TP); 4: North China; 5: South China; 6: East China Sea; 7: Korea–Japan] are defined by red boxes for analysis. Values in gray boxes denote percentages of dust emission, transport, and deposition to total dust mass. Emis.: dust emission; Tran.: dust transport; Dry Dep.: dry deposition; Wet Dep.: wet deposition.

altitude westerly jet with suitable vertical circulation is the main cause of the higher wind speeds in the middle and lower troposphere over the GD, which leads to GD dust being more susceptible to uplift and long-range transport. Therefore, the GD plays a more important role than the TD in terms of dust transport over continental China. Compared with GD dust, TD dust is not easily transported out of the basin because of its lower elevation, complex topography, and low wind speeds in the upper atmosphere, although the TD has the largest dust emission flux in East Asia. However, TD dust is still the predominant contributor to the dust transported over long distances when uplifted to high altitudes (> 5000 m) (Sun et al., 2001; Shi et al., 2012; Chen et al., 2016).

## 4. Climatic effect of EAD

East Asia experiences high dust concentrations, which may result in substantial effects on the energy budget and climate change via the "direct" and "indirect" effects of dust (Wang et al., 2005; Huang et al., 2006c; Liao et al., 2009). However, the overall climatic effects of dust can vary greatly among regions because of the complex nonlinear interplay between dust aerosols and climate systems. The climatic effect of EAD has rarely been explored. The direct and indirect effects of EAD remain one of the largest uncertainties in climate models. In this section, we focus on the climate change induced by EAD in the atmosphere and in snow, and further investigate its influences on a series of important physical quantities, such as atmospheric stability, cloud lifetimes, and precipitation efficiency.

### 4.1 *RF of dust over East Asia*

Dust direct radiative forcing (DDRF) over East Asia accounts for about 42% of the total aerosol forcing, which plays an important role in the radiation budget and regional climate. Studies of DDRF over East Asia have been conducted since the 1990s. Numerical models have been used in combination with broadband radiation observations, sun photometer readings, and lidar measurements associated with satellite retrievals, to predict the spatiotemporal variability of DDRF over East Asia (Wang et al., 2004; Zhang H. et al., 2009a, b, 2010, 2012; Wang W. C. et al., 2010). Generally, the uncertainties in DDRF over East Asia derive mainly from the following two causes. First, biases from dust emission, chemical transformation, dust transport, and removal processes of dust, greatly affect the precision of DDRF assessments. Second, differences in the particle size distribution, vertical distribution of the dust layer, absorptive characteristics, chemical composition, particle shape, and environmental conditions (e.g., surface albedo, solar zenith angle, and cloud height) can lead to large heterogeneities in the quantitative assessment of DDRF (Sokolik and Toon, 1996; Tegen et al., 1996; Takemura et al., 2003; Wang et al., 2004, 2007; Wu et al., 2004). Therefore, more observational data of dust optical properties over East Asia were used to develop dust models.

Takemura et al. (2003) coupled the SPRINTARS model with a 3-D aerosol transport–radiation model to simulate the DDRF over East Asia, based on observations from the APEC and ACE-Asia field campaigns (see Table 1). The imaginary part of the refractive index of soil dust was modified from 0.08 to 0.002 at the visible wavelength in the model, which agreed closely with the simulation and observation of single scattering albedo in the dust layer. Moreover, Wang et al. (2004) noted that EAD particles absorb less solar radiation than Saharan dust particles. Furthermore, the authors included the dust refractive index and dust size distribution from Cele (37°01′N, 80°44′E) in the TD in the radiative transfer model (Shi, 1984) and calculated the average DDRF over East Asia under clear-sky conditions (see Table 1). They further calculated the radiative heating rate of EAD from the deserts of China to the North Pacific Ocean using the same radiative transfer model (Wang et al., 2007). Huang et al. (2009) also used the Fu–Liou radiation model in combination with various surface observation data to investigate the EAD heating rate (Table 1).

In addition, separation of chemistry and meteorology increases the uncertainty in dust simulations (Grell et al., 2005). In recent years, increasing attention has been paid to online dust modeling, in which the feedbacks between dust and radiation were examined (Zhang et al., 2003; Wu et al., 2004; Zhao et al., 2008; Wang H. et al., 2010; Grell and Baklanov, 2011). More studies focusing on dust radiative and climate effects over East Asia have been conducted using two-way online coupled regional dust modeling (Wang H. et al., 2010; Zhao et al., 2011; Chen et al., 2013, 2014a). Han et al. (2010) incorporated aerosol and gas chemistry modules into RIEMS (Regional Integrated Environmental Model System), based on MM5 (version 5 of the NCAR's Mesoscale Model), and developed a new online coupled regional climate–chemistry–aerosol model (RIEMS-Chemaero). The dust emission flux was calculated for each size bin, while dust deflation was treated empirically based on several factors (e.g., threshold friction velocity, relative humidity, and the reduction factor of vegetation). This model was firstly applied to investigate the dust RF and transport of an extremely intense dust storm over East Asia (Han et

**Table 1.** Summary of dust's direct radiative forcing over East Asia, based on numerical model simulations in previous studies

| TOA (W m$^{-2}$) | ATM (W m$^{-2}$) | BOT (W m$^{-2}$) | Region | Time | Method | Reference |
|---|---|---|---|---|---|---|
| –3 (SW) | – | –17 (SW) | 20°–50°N, 100°–150°E | 5–15 April 2001 | CFORS model coupled with a Monte Carlo radiative transfer model[1] | Conant et al. (2003) |
| Clear sky/at tropopause: –0.63 (SW) +0.44 (LW) –0.19 (Total) | – | Clear sky: –1.93 (SW) +0.86 (LW) –1.07 (Total) | 15°–52°N, 90°–152°E | April 2001 | SPRINTARS model including Spectral Radiation-Transport | Takemura et al. (2003) |
| Whole sky/at tropopause: –0.32 (SW) +0.31 (LW) –0.02 (Total) | – | Whole sky: –1.57 (SW) +0.27 (LW) –1.10 (Total) | | | | |
| –1.70 (SW) +0.76 (LW) –0.94 (Total) | – | –6.25 (SW) +0.76 (LW) –5.44 (Total) | 16°–70°N, 75°–225°E | Spring 2001 | Radiative transfer model developed by Guangyu Shi | Wang et al. (2004) |
| – | – | –17.5 | Gosan super-site, South Korea (33°17′N, 126°10′E) | 11–27 April 2001 | Fu–Liou radiative transfer model | Kim et al. (2006) |
| –0.90 | 0.6 | –1.50 | 0°–50°N, 70°–150°E | March 2002 | NCAR CCM3 CRM coupled with ADAM and aerosol dynamic model | Park and Jeong (2008) |
| 44.4 | 86.3 | –41.9 | Taklimakan Desert | July 2006 | Fu–Liou radiative transfer model | Huang et al. (2009) |
| –5 | – | –15 | East Asian deserts | FMAM[2] 1997–2006 | RegCM3[3] | Zhang H. et al. (2009a) |
| 0.94 (SW: 0.48; LW: 0.45) | – | –3.93 (SW: –6.09; LW: 2.16) | 15°–55°N, 75°–145°E | 19–22 March 2010 | RIEMS-Chemaero[4] | Han et al. (2012) |
| 1.18 (SW: 0.40; LW: 0.78) | – | –8.42 (SW: –12.55; LW: 4.13) | Eastern China | | | |
| 1.40 (SW: 0.67; LW: 0.73) | – | –6.09 (SW: –11.9; LW: 5.82) | Western China | | | |
| – | – | Up to –90 (SW); up to 40 (LW) | Gobi Desert | | | |
| –13.6 (SW) | 23.2 (SW) | –36.8 (SW) | Yangtze Delta of China | 14–17 March and 25–26 April 2009 | SBDART model[5] | Liu et al. (2011) |
| 5.93–35.7 | 16.77–56.32 | –6.3 to –30.94 | Minqin (36.61°N, 102.96°E), SACOL (36.61°N, 102.96°E) | 24–30 April 2010 | Fu–Liou radiative transfer model | Wang Z. L. et al. (2013) |
| Up to –8 (SW); up to 2 (LW) | – | Up to –25 (SW); up to 8 (LW) | East Asian deserts | Spring and summer of 2000–09 | RegCM4[6] | Sun et al. (2012) |
| –3.97 | 1.61 | –5.58 | Tibetan Plateau | 26–30 July 2006 | WRF-Chem coupled with RRTMG radiative model | Chen et al. (2013) |

[1]A three-dimensional atmospheric chemical transport model [Chemical Weather Forecast System (CFORS)];
[2]February–March–April–May (FMAM);
[3]Regional Climate Model Version 3 (RegCM3);
[4]RIEMS-Chemaero represents an online-coupled regional climate–chemistry–aerosol model;
[5]Santa Barbara DISORT Atmospheric Radiative Transfer model (SBDART model);
[6]Regional Climate Model Version 4 (RegCM4).

al., 2012, 2013). Wang H. et al. (2010) also developed a new radiative scheme within a two-way dust modeling procedure (integrating dust prediction and radiative effects) to investigate the DDRF over East Asia. The updated data on land desertification, land surface, soil texture, and dust optical properties over China's mainland were used. Chen et al. (2014b) applied the Rapid Radiative Transfer Model (RRTMG) to both shortwave (SW) and longwave (LW) radiation in WRF-Chem to calculate the DDRF over East Asia (Fig. 5). The authors believed that the online estimation of direct dust effects improved the prediction of meteorological variables (e.g., temperature, pressure, and wind) for the dust events. Moreover, these studies included LW radiation in the radiative scheme, which significantly decreased the biases in radiative budget estimation.

### 4.2 *Climatic impact induced by direct and indirect/semi-direct effect of EAD in the atmosphere*

In addition to the direct effect of EAD on SW and LW radiation, the indirect effect of dust can modify the microphysical properties of clouds (e.g., cloud liquid water

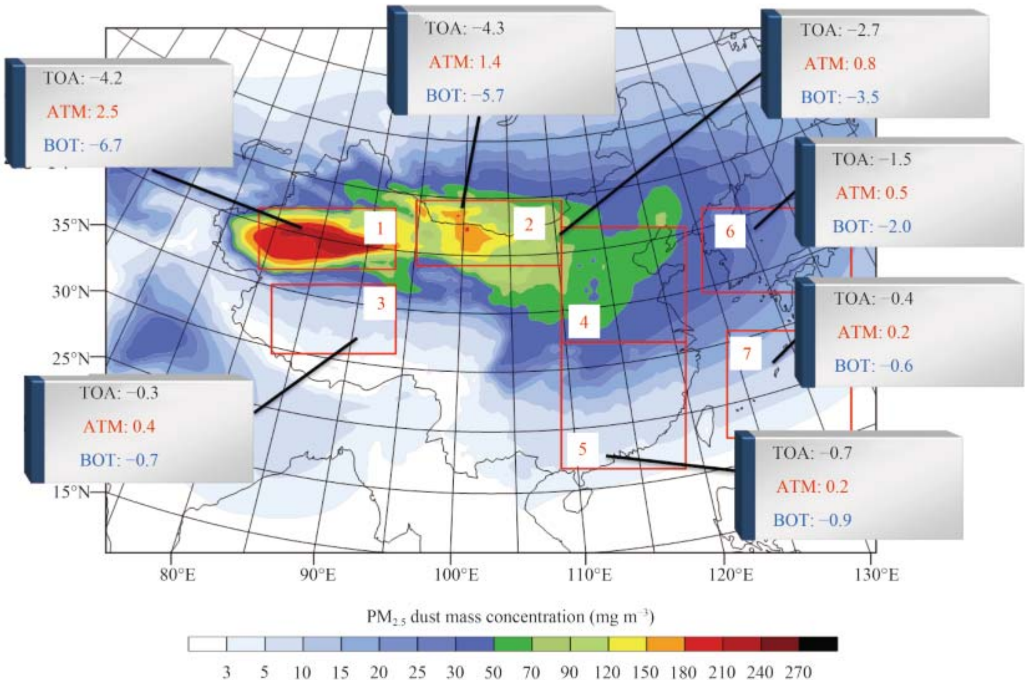


**Fig. 5.** As in Fig. 4, but the gray boxes show values for the dust radiative forcing (W $m^{-2}$) at the TOA (top of the atmosphere), in the ATM (atmosphere), and at the BOT (surface), in 2007–11, based on WRF-Chem simulations. A positive value indicates downward forcing for the TOA and surface, and absorption/heating for the atmosphere.

content, cloud fraction, cloud particle size), as dust particles are efficient cloud condensation nuclei (CCN) and ice nuclei (IN), and further influence the precipitation efficiency. Yin et al. (2002) performed numerical simulations with a 2D nonhydrostatic cloud model with detailed microphysics to investigate the impacts of dust particles on development of cloud and precipitation. Their results indicated that dust particles can enhance the formation of rain droplets in continental clouds, while they have a small impact on precipitation in maritime clouds.

The semi-direct effect involves dust particles absorbing solar radiation, which can be re-emitted as thermal radiation to heat the atmosphere, thus enhancing the evaporation of cloud droplets (Han et al., 2013). Using a dynamic cloud model with detailed microphysics of both warm- and ice-phase processes, Yin and Chen (2007) found that the dust layer at the cloud-base height and below 3 km could induce heating, suppress the formation of cloud droplets, and reduce cloud optical depth. In addition, dust particles within or above the clouds are likely to evaporate cloud droplets over the arid and semi-arid regions (Huang et al., 2006b, 2010; Wang W. C. et al., 2010; Zhao S. et al., 2015).

Combined with dust direct and indirect/semi-direct effects, many studies on the climate change induced by EAD have been conducted. Results show clear decreases in surface temperature accompanied by reduced sensible heat flux due to the scattering and absorption of solar radiation by dust particles (Wu et al., 2010; Wei and Zhang, 2011; Zhao S. et al., 2014). Moreover, the diurnal temperature range (DTR), as an important indicator of the climatic system, can reflect climatic anomalies well. Can mineral dust significantly influence the DTR over East Asia? How do dust aerosols contribute to the DTR variations? To address these questions, we employed the WRF-Chem model. Our results (Fig. 6) showed that dust aerosol could play a role in changing the DTR through modification of the surface energy balance, directly or through its impact on cloud properties, soil moisture, and snow cover over East Asia. Changes in DTR over East Asia induced by dust aerosol result from the diurnal asymmetry of surface temperature; that is, the maximum temperature ($T_{max}$) changes obviously while the minimum temperature ($T_{min}$) remains constant or is modified slightly (Fig. 6). The annual mean $T_{max}$ and $T_{min}$ decrease by 0.54 and 0.23°C, respectively, and the DTR decreases by 0.31°C, with the pattern similar to that of $T_{max}$. The largest reduction in DTR, by up to 0.37°C, happened in springtime, which is the main period of dust production over East Asia.

In the daytime, the dust layers in the atmosphere can strongly absorb and scatter SW radiation, which reduces the amount of SW radiation reaching the ground. Dust direct RF is negative because the SW cooling effect of dust outweighs the LW warming effect. The $T_{max}$ is dominated by surface SW solar radiation induced by dust. At nighttime, the SW RF of dust turns zero. The dust layers in the atmosphere can increase the LW radiation reaching the surface and induce a slight warming effect on surface temperature. However, the indirect effect of dust reduces the surface temperature through changing cloud fractions. Overall, dust reduces the surface temperature at nighttime, since the cooling effect caused by the dust indirect effect outweighs the LW warming effect of dust.

The cross-correlation coefficients of the changes in cloud water content, snow cover, soil moisture, precipitation, daily maximum temperature, daily minimum temperature, and DTR induced by EAD were calculated in this study. The correlation coefficient between the DTR and daily maximum temperature reached 0.68, while it was 0.15 between DDRF and daily minimum temperature. The variation in cloud water content and snow cover was closely related to the DTR, and the correlation coefficient reached –0.70 and –0.58, respectively, which indicated that the dust could indirectly affected the ground DTR by changing the cloud cover and snow cover over East Asia. EAD can accelerate the melting of snow on the TP and parts of North China, and reduce the snow cover in the area due to the dust absorption. The melting of snow weakened the surface albedo, and thus increased the DTR in the TP and parts of North China.

Precipitation responses induced by dust particles also vary in different areas and in different seasons. Guo and Yin (2015) investigated the impacts of EAD on the precipitation, summer monsoon, and sea surface temperature over East Asia using a regional coupled atmosphere–ocean–land model, i.e., the Regional Integrated Environment Model System (RCM RIEMS 2.0). The indication was that dust-induced atmospheric heating and surface cooling reduced precipitation by 0.03 mm day$^{-1}$ in spring and increased precipitation by 0.28 mm day$^{-1}$ in summer over East Asia. The simulation results also indicated that dust aerosol could weaken the East Asia summer monsoon by reducing the land–sea temperature contrast. Wu et al. (2010) pointed out that EAD helps to partly offset the "southern flood and northern drought" pattern in China, if only considering the direct effects of EAD. Sun et al. (2012) also found that the direct effect of EAD might lead to suppressed precipitation in the downwind areas (Northwest China and East China Sea) and enhance precipitation around its source. Moreover, as revealed in these studies, the "elevated heat pump" effect generated by the TP dust could alter moisture, cloud, and deep convection in northern India, which accelerated the snowmelt in the Himalayas, hence resulting in an earlier onset and intensification of the Indian summer monsoon. The increased rainfall in India, combined with the large-scale pressure anomaly pattern at sea level, led to a northwestward shift of the rainbelt over East Asia and adjacent regions (Lau et al., 2006; 2010; Huang et al., 2007; Qian et al., 2009, 2015).

More recently, Gu et al. (2016) investigated the precipitation responses induced by dust in North Africa, South Asia, and East Asia using an atmospheric general circulation model. The direct and semi-direct effects of dust were considered in the simulation. Dust over the Saharan Desert enhances the upward motion and strengthens the cyclonic circulation to its south where precipitation occurs, leading to decreased precipitation over the Sahel regions and the tropical North Atlantic. The thermal and dynamic effects of East/South Asian dust correspond with North Africa. However, it differs in that dust particles are located in the upper troposphere over the major rainfall areas in South/East Asia, except southeastern China. The increasing upward motion and

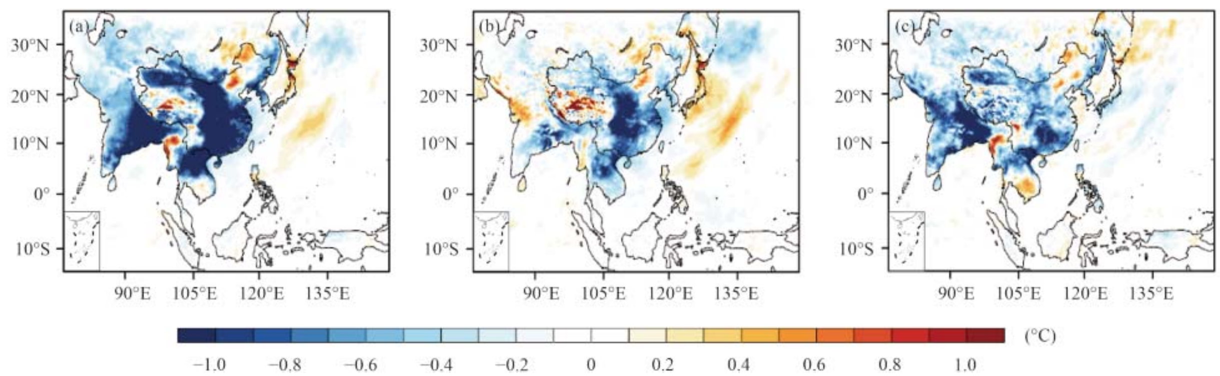


**Fig. 6.** Annual dust-induced change in (a) maximum temperature, (b) minimum temperature, and (c) diurnal temperature range change at 2 m over East Asia from the WRF-Chem simulation in 2010.

strengthened cyclonic circulation induced by dust aerosols lead to increased precipitation intensity and variability. As for southeastern China, where the monsoon regions are located, precipitation decreases during the premonsoon season because the dust layer is located to the north of it, which induces anomalously weakened upward motion of the atmosphere over southeastern China. The precipitation and cloud in southeastern China increase during the monsoon season because the stronger monsoon flow induced by dust aerosols bring moister and warmer air, although there is no obvious change in dust concentrations over these regions (Wu et al., 2013; Gu et al., 2016) (Fig. 7).

### 4.3 *Climatic impact of EAD in seasonal snow*

Snow is the most reflective natural surface on the earth. Small changes in snow albedo can greatly affect surface warming due to rapid feedbacks from changes in snow morphology, sublimation, and melting rates. Results have shown that the snow albedo, particularly within the visible bands, can be influenced by light-absorbing impurities deposited on or in the snowpack (Flanner et al., 2007, 2012; Wang et al., 2014). In recent years, a number of modeling studies have indicated that the RF from black carbon (BC) in snow has been an important anthropogenic forcing for climate change during the past century (Lau et al., 2008, 2010; Ming et al., 2008; Qian et al., 2009, 2015; Xu et al., 2009, 2012; Cong et al., 2013). These studies illustrate that dust in snow causes a remarkable decline in its albedo, especially within the visible bands, which could have a significant effect on the atmospheric general circulation and hydrological cycle (Qian et al., 2009, 2015; Liu et al., 2013; Kuchiki et al., 2015). Kuchiki et al. (2015) further observed that the maximum dust mass concentration in surface snow in Japan was 260 ppmw, much larger than that of elemental carbon and organic carbon (OC) mass concentrations because (1) dust mass loading in the atmosphere is much larger than BC and OC, and (2) dust particles are more sensitive to dry deposition and melt amplification. Therefore, the radiative effect of dust in snow cannot be ignored in dust modeling.

The Snow, Ice, and Aerosol Radiation (SNICAR) model was developed by Flanner et al. (2007) to investigate the impact of light-absorbing aerosols on snow properties. This model applies the two-stream multilayer radiative approximation of Toon et al. (1989) for the radiative transfer solution, and theory from Warren and Wiscombe (1980) for estimating the albedo of pure or contaminated snow. Snow within the model is regarded as ice spheres following a log-normal distribution. The optical properties of aerosols and ice crystals are derived with Mie solutions. Dust particles are divided into four size bins to estimate the optical properties based on the Maxwell–Garnett approximation, with an assumption for ingredients of dust particles. This approach helps to better understand the dust RF in snow, one of the largest sources of uncertainty in the assessment of aerosol RF in climate change (Hansen et al., 1997; Aoki et al., 2006; Painter et al., 2007).

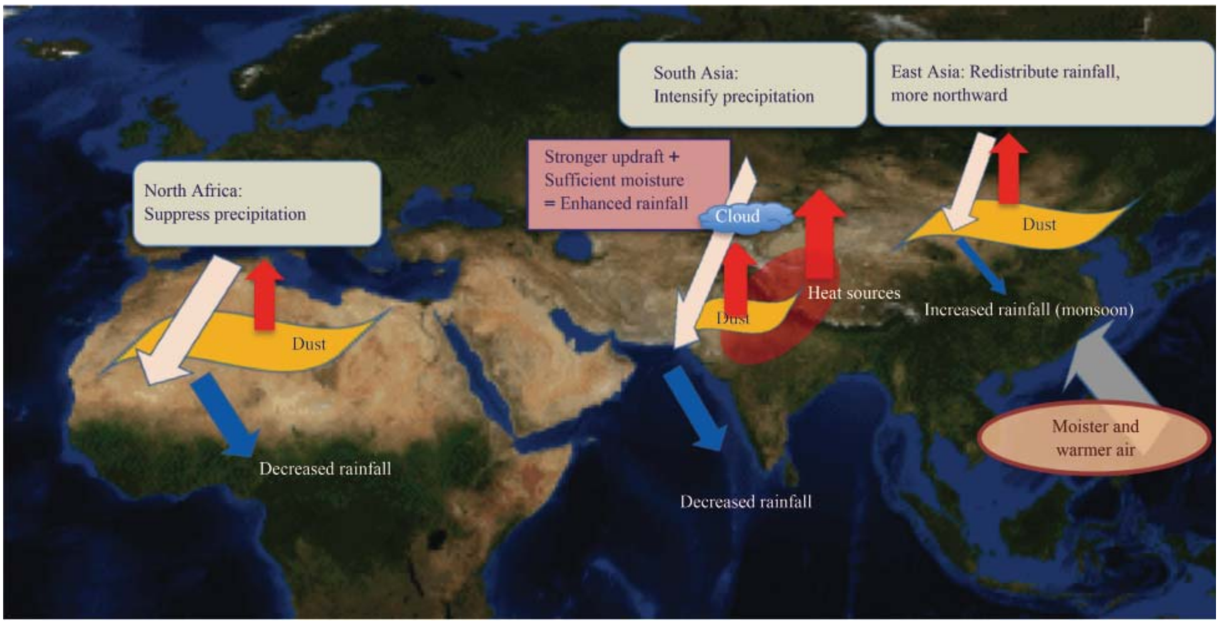


**Fig. 7.** Schematic representation of dust influences in North Africa, South Asia, and East Asia.

Dust in snow in different regions produces distinct radiative feedback. Therefore, observational studies of dust in snow over East Asia are necessary. Observational datasets of dust concentrations in midlatitude seasonal snow have been scarce. Many projects have been conducted to explore light-absorbing impurities in snow (Huang et al., 2011). Five field campaigns were conducted in 7 provinces in China from 2010 to 2014. These studies provided valuable observations of the albedo of seasonal snow in China. The results of these campaigns were reported by Huang et al. (2011) and Wang X. et al. (2013). Based on these observational results, Zhao C. et al. (2014) coupled the SNICAR model (Flanner et al., 2007, 2012) with WRF-Chem, including sophisticated representation of snow metamorphism processes to simulate the RF of dust in seasonal snow over northern China. The study evaluated the simulated EAD in snow at a relatively high spatial resolution against field campaigns. The results showed that dust and BC mass concentrations in snow induced a similar magnitude of radiative warming (approximately 10 W $m^{-2}$) in the snowpack, comparable to the magnitude of radiative cooling at the surface induced by absorbed aerosols in the atmosphere (Fig. 8).

Dust in snow over the TP has attracted considerable interest because its role in climate change can hardly be overstated. The averaged RF of dust in snow over the TP can increase from 1.1 to 8.6 W $m^{-2}$, exceeding the RF of BC in snow, during the melting seasons in the Zhadang Glacier. This can reduce the albedo of glaciers (also called the "dirtying" or "darkening" effect), exacerbate the mass loss of glaciers in the inner TP (Qu et al., 2014), and substantially change the surface albedo and radiative fluxes over East Asia (Qian et al., 2009). However, how do TP dust aerosols in snow impact the hydrological cycle on the TP, and even the monsoon climate over East Asia? Additional studies are needed to examine the impacts of TP dust, through direct and indirect effects, on snow, and hence its impacts on climate and the hydrological cycle.

## 5. Concluding remarks

### 5.1 *Uncertainties in EAD simulations*

East Asia is one of the largest dust source regions in the world. EAD modulates the energy balance and climate feedback through its influence on solar and terrestrial radiation, cloud properties, and precipitation on both regional and global scales. Detailed investigations of the life cycle and associated climate impacts of EAD are imperative because of its environmental, climatic, and geochemical importance. In this review, we summar-

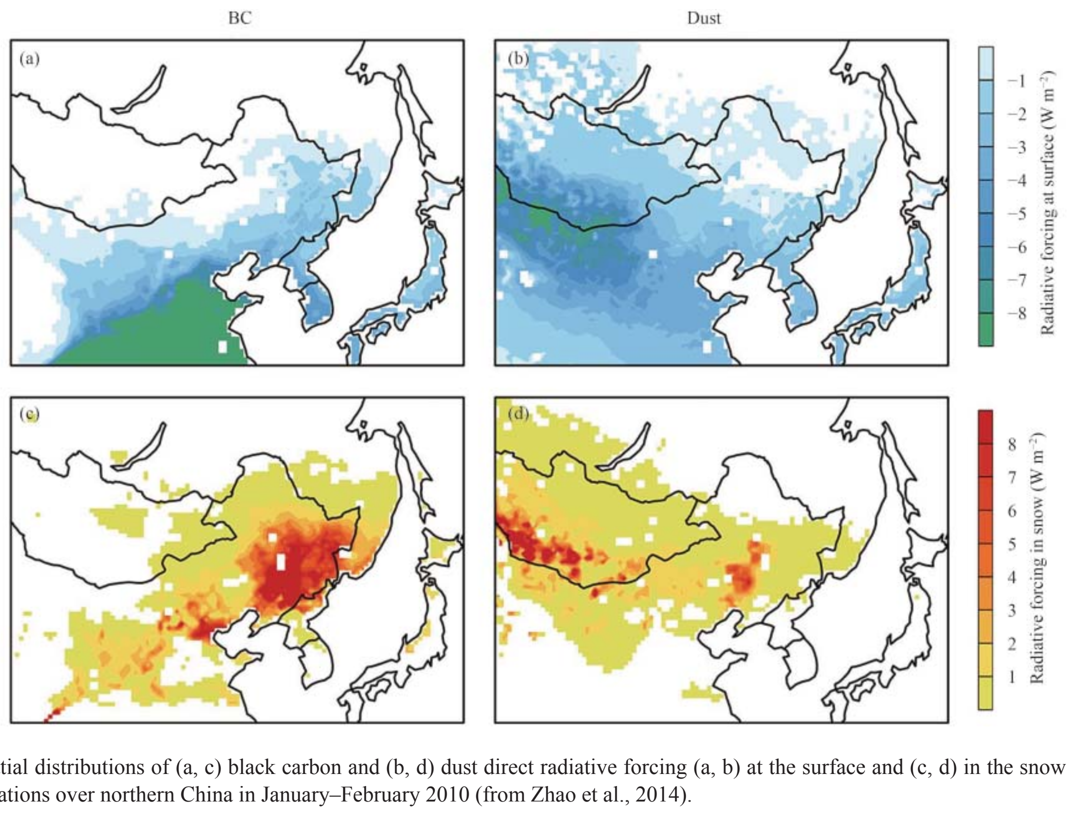


**Fig. 8.** Spatial distributions of (a, c) black carbon and (b, d) dust direct radiative forcing (a, b) at the surface and (c, d) in the snow from WRF-Chem simulations over northern China in January–February 2010 (from Zhao et al., 2014).

ized the achievements and progress in studies of the life cycle and associated DDRF and climate impacts of EAD over East Asia using numerical modeling. However, knowledge of the EAD's dust cycle and interactions with other biogeochemical cycles is far less complete than that for other dust source regions (e.g., the Sahara Desert). Many uncertainties and challenges in EAD simulations remain. Some crucial feedback mechanisms by which EAD modulates the cloud properties, cloud lifetimes, and rain formation are still under debate and highly uncertain.

Compared with other regions such as the Sahara Desert and North American deserts, accurate EAD simulations with a regional or global model still faces great challenges. Uncertainties in EAD modeling exist in various aspects as follow: (1) lack of systematic observation of dust aerosols from ground-based networks, aircraft observations, and satellite retrievals; (2) inaccurate description of dust emission, long-term transport, and dry/wet deposition in numerical models; and (3) poor understanding of the aggregation, coagulation, and heterogeneous chemical reaction of dust particles.

Moreover, large uncertainties also exist in physical parameterizations, including those for emission, cloud microphysics, planetary boundary layer, and convection (e.g., Yang et al., 2012, 2013; Zhao et al., 2013a; Yan et al., 2014). Zou et al. (2014) and Yang et al. (2015a, b) showed that parametric uncertainties in cloud and precipitation processes in both regional and global climate models can evidently affect the simulations of cloud, precipitation, radiation, and circulation over the East Asian summer monsoon region. These could further influence the dust climatic effects because of the uncertainties associated with the simulated transport, radiative, and microphysical effects of dust. Therefore, the process by which dust acts as CCN or IN remains one of the most poorly understood issues for establishing a clear causal relationship between dust and precipitation. Substantial knowledge gaps in modeling the impacts of dust on clouds and precipitation over East Asia remain.

### 5.2 *Future*

EAD emission, transport, and radiative effects have received deserved attention in studies of radiative budget and climate change of the earth system. However, we also want to point out several directions in future research.

(1) The development of integrated systematic observations of EAD, especially the dust emission flux, dust dry/wet deposition, vertical structure of dust layers, aerosol size distribution, and dust mass concentrations in snow, is important for improving the dust modeling. More specifically, powerful satellite retrievals (e.g., CALIOP), advanced instruments (e.g., ground-based lidar networks), and *in situ* measurements [e.g., the Aerosol Robotic Network (AERONET) and SACOL] are needed over East Asia to evaluate dust modeling results. Currently, barriers exist between observations and numerical models because of differences in research methods and technical backgrounds. Modeling studies have always passively accepted observed results but seldom considered observation errors and inverse problems of observations because of incomprehension regarding the principles and technical performances of instruments and observation methods. Observational studies have focused on revealing these phenomena but have often ignored some key parameters of dust modeling. Because of these inhibitors, the joint development of observational techniques and dust modeling is critical to EAD parameterizations (e.g., dust emission, dust deposition, radiation schemes, and land surface processes).

(2) Dust aerosols have various sources from both natural and anthropogenic processes (Tegen and Fung, 1994; Zender et al., 2003). All current studies of dust emission parameterization schemes have mainly focused on natural dust. Anthropogenic dust originates from human activities through modifying or disturbing soil, such as by agriculture, livestock herding, construction, and off-road vehicle use. Huang et al. (2015) found that anthropogenic dust accounts for more than 91.8%, 76.1%, and 73.9% of the total dust emission in East China, India, and North America, respectively (Fig. 9). Natural or anthropogenic dust plays an important role in the radiative budget and hydrological cycle. Therefore, developing an emission scheme for anthropogenic dust aerosols in numerical models is necessary for objective assessment of

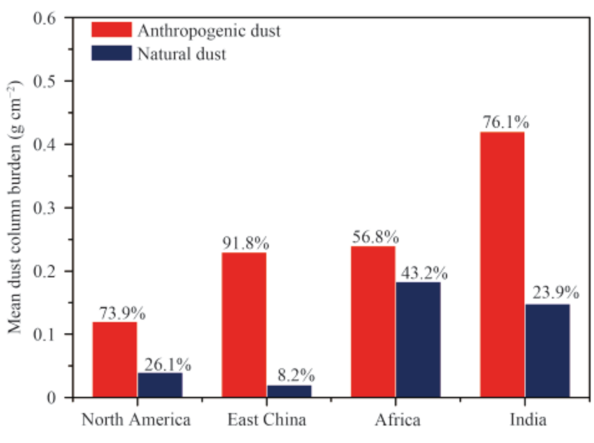


**Fig. 9.** Relative percentage (%) of natural dust and anthropogenic dust to total dust in North America, East China, Africa, and India. The figure is plotted based on the data from Huang et al. (2015).

the attribution of climate change.

(3) Huge uncertainties exist in the estimation of precipitation responses induced by EAD in model simulations. An increasing number of studies have noted that precipitation change is induced by dust from two aspects: surface cooling, which may reduce rainfall, and the heating of the atmosphere, which may enhance rainfall. Dust induces the redistribution of precipitation in different regions and different periods, rather than simply acts to increase or decrease precipitation. Most previous studies have investigated the climatic effect of dust by only considering dust direct effects. However, dust can also affect cloud properties and then climate through acting as IN in heterogeneous ice nucleation processes. The effect of EAD IN needs to be investigated as well.

***Acknowledgments***. We appreciate the comments by Professor Hua Zhang and the two anonymous reviewers, which have helped improve the paper.

## REFERENCES

Ai, N., and K. R. Polenske, 2008: Socioeconomic impact analysis of yellow-dust storms: An approach and case study for Beijing. *Economic Systems Research*, **20**, 187–203, doi: 10.1080/09535310802075364.

Aoki, T., H. Motoyoshi, Y. Kodama, et al., 2006: Atmospheric aerosol deposition on snow surfaces and its effect on albedo. *SOLA*, **2**, 13–16, doi: 10.2151/sola.2006-004.

Bi, J. R., J. P. Huang, Q. Fu, et al., 2011: Toward characterization of the aerosol optical properties over Loess Plateau of northwestern China. *J. Quant. Spectros. Radiative Transfer*, **112**, 346–360, doi: 10.1016/j.jqsrt.2010.09.006.

Bian, H., X. X. Tie, J. J. Cao, et al., 2011: Analysis of a severe dust storm event over China: Application of the WRF-dust model. *Aerosol and Air Quality Research*, **11**, 419–428, doi: 10.4209/aaqr.2011.04.0053.

Chao, W.-L., and M. Alexander, 1984: Mineral soils as carriers for *Rhizobium inoculants*. *Appl. Environ. Microbio.*, **47**, 94–97.

Chen, S. Y., J. P. Huang, J. J. Liu, et al., 2010: Effects of dust aerosols on cloud in semi-arid regions as inferred from OMI and MODIS retrievals. *Adv. Earth Sci.*, 25, 188–198. (in Chinese)

Chen, S. Y., J. P. Huang, C. Zhao, et al., 2013: Modeling the transport and radiative forcing of Taklimakan dust over the Tibetan Plateau: A case study in the summer of 2006. *J. Geophys. Res*, **118**, 797–812, doi: 10.1002/jgrd.50122.

Chen, S. Y., C. Zhao, Y. Qian, et al., 2014a: Regional modeling of dust mass balance and radiative forcing over East Asia using WRF-Chem. *Aeolian Research*, **15**, 15–30, doi: 10.1016/j.aeolia.2014.02.001.

Chen, S. Y., J. P. Huang, Y. Qian, et al., 2014b: Effects of aerosols on autumn precipitation over mid–eastern China. *J. Trop. Meteor.*, **20**, 242–250.

Chen, S. Y., J. P. Huang, L. T. Kang, et al., 2016: Emission, transport and radiative effects of mineral dust from Taklimakan and Gobi deserts: Comparison of measurements and model results. *Atmos. Chem. Phys.*, doi: 10.5194/acp-2016-531.

Chen, S. Y., J. P. Huang, J. Li, et al., 2017: Comparisons of dust emission, transport, and deposition between the Taklimakan desert and Gobi desert from 2007 to 2011. *Sci. China Earth Sci*, doi: 10.1007/s11430-016-9051-0.

Conant, W. C., J. H. Seinfeld, J. Wang, et al., 2003: A model for the radiative forcing during ACE-Asia derived from CIRPAS Twin Otter and R/V *Ronald H. Brown* data and comparison with observations. *J. Geophys. Res.*, **108**, doi: 10.1029/2002JD003260.

Cong, Z. Y., S. C. Kang, S. P. Gao, et al., 2013: Historical trends of atmospheric black carbon on Tibetan Plateau as reconstructed from a 150-year lake sediment record. *Environ. Sci. Technol.*, **47**, 2579–2586, doi: 10.1021/es3048202.

Eguchi, K., I. Uno, K. Yumimoto, et al., 2009: Trans-Pacific dust transport: Integrated analysis of NASA/CALIPSO and a global aerosol transport model. *Atmos. Chem. Phys.*, **9**, 3137–3145, doi: 10.5194/acp-9-3137-2009.

Fairlie, T. D., D. J. Jacob, J. E. Dibb, et al., 2010: Impact of mineral dust on nitrate, sulfate, and ozone in trans-Pacific Asian pollution plumes. *Atmos. Chem. Phys.*, **10**, 3999–4012, doi: 10.5194/acp-10-3999-2010.

Flanner, M. G., C. S. Zender, J. T. Randerson, et al., 2007: Present-day climate forcing and response from black carbon in snow. *J. Geophys. Res.*, **112**, D11202, doi: 10.1029/2006JD008003.

Flanner, M. G., X. Liu, C. Zhou, et al., 2012: Enhanced solar energy absorption by internally-mixed black carbon in snow grains. *Atmos. Chem. Phys.*, **12**, 4699–4721, doi: 10.5194/acp-12-4699-2012.

Fu, Q., T. J. Thorsen, J. Su, et al., 2009: Test of Mie-based single-scattering properties of non-spherical dust aerosols in radiative flux calculations. *J. Quant. Spectros. Radiative Transfer*, **110**, 1640–1653, doi: 10.1016/j.jqsrt.2009.03.010.

Fu, X., S. X. Wang, Z. Cheng, et al., 2014: Source, transport, and impacts of a heavy dust event in the Yangtze River Delta, China, in 2011. *Atmos. Chem. Phys.*, **14**, 1239–1254, doi: 10.5194/acp-14-1239-2014.

Ge, J. M., J. P. Huang, J. Su, et al., 2011: Shortwave radiative closure experiment and direct forcing of dust aerosol over northwestern China. *Geophys. Res. Lett.*, **38**, L24803, doi: 10.1029/2011GL049571.

Ginoux, P., M. Chin., I. Tegen, et al., 2001: Sources and distributions of dust aerosols simulated with the GOCART model. *J. Geophys. Res.*, **106**, 20255–20274, doi: 10.1029/2000JD000053.

Gong, S. L., X. Y. Zhang, T. L. Zhao, et al., 2003a: Characterization of soil dust aerosol in China and its transport and distribution during 2001 ACE-Asia. 2: Model simulation and validation. *J. Geophys. Res.*, **108**, doi: 10.1029/2002JD002633.

Gong, S. L., L. A. Barrie, J. P. Blanchet, et al., 2003b: Canadian aerosol module: A size segregated simulation of atmospheric aerosol processes for climate and air quality models 1. Module development. *J. Geophys. Res.*, **108**, AAC 3-1–AAC 3-16, doi: 10.1029/2001JD002002.

Gong, S. L., X. Y. Zhang, T. L. Zhao, et al., 2006: A simulated climatology of Asian dust aerosol and its trans-Pacific transport. Part II: Interannual variability and climate connections. *J. Climate*, **19**, 104–122, doi: 10.1175/JCLI3606.1.

Grell, G. A., S. E. Peckham, R. Schmitz, et al., 2005: Fully coupled “online” chemistry within the WRF model. *Atmos. Environ.*, **39**, 6957–6975, doi: 10.1016/j.atmosenv.2005.04.027.

Grell, G., and A. Baklanov, 2011: Integrated modeling for forecasting weather and air quality: A call for fully coupled approaches. *Atmos. Environ.*, **45**, 6845–6851, doi: 10.1016/j.atmosenv.2011.01.017.

Gu, Y., Y. Xue, F. D. Sales, et al., 2016: A GCM investigation of dust aerosol impact on the regional climate of North Africa and South/East Asia. *Climate Dyn.*, **46**, 2353–2370, doi: 10.1007/s00382-015-2706-y.

Guo, J., and Y. Yin, 2015: Mineral dust impacts on regional precipitation and summer circulation in East Asia using a regional coupled climate system model. *J. Geophys. Res.*, **120**, 10378–10398, doi: 10.1002/2015JD023096.

Han, Z. W., 2010: Direct radiative effect of aerosols over East Asia with a regional coupled climate/chemistry model. *Meteor. Z.*, **19**, 287–298, doi: 10.1127/0941-2948/2010/0461.

Han, Z. W., H. Ueda, K. Matsuda, et al., 2004: Model study on particle size segregation and deposition during Asian dust events in March 2002. *J. Geophys. Res.*, **109**, doi: 10.1029/2004JD004920.

Han, Z. W., J. W. Li, X. G. Xia, et al., 2012: Investigation of direct radiative effects of aerosols in dust storm season over East Asia with an online coupled regional climate–chemistry–aerosol mode. *Atmos. Environ.*, **54**, 688–699, doi: 10.1016/j.atmosenv.2012.01.041.

Han, Z. W., J. W. Li, W. D. Guo, et al., 2013: A study of dust radiative feedback on dust cycle and meteorology over East Asia by a coupled regional climate–chemistry–aerosol model. *Atmos. Environ.*, **68**, 54–63, doi: 10.1016/j.atmosenv.2012.11.032.

Hansen, J., M. Sato, and R. Ruedy, 1997: Radiative forcing and climate response. *J. Geophys. Res.*, **102**, 6831–6864, doi: 10.1029/96JD03436.

Hsu, S. C., F. Tsai, F.-J. Lin, et al., 2013: A super Asian dust storm over the East and South China Seas: Disproportionate dust deposition. *J. Geophys. Res.*, **118**, 7169–7181, doi: 10.1002/jgrd.50405.

Huang, J. P., B. Lin, P. Minnis, et al., 2006a: Satellite-based assessment of possible dust aerosols semi-direct effect on cloud water path over East Asia. *Geophys. Res. Lett.*, **33**, doi: 10.1029/2006GL026561.

Huang, J. P., Y. J. Wang, T. H. Wang, et al., 2006b: Dusty cloud radiative forcing derived from satellite data for middle latitude regions of East Asia. *Progress in Natural Science*, **16**, 1084–1089, doi: 10.1080/10020070612330114.

Huang, J. P., P. Minnis, B. Lin, et al., 2006c: Possible influences of Asian dust aerosols on cloud properties and radiative forcing observed from MODIS and CERES. *Geophys. Res. Lett.*, **33**, L06824, doi: 10.1029/2005GL024724.

Huang, J. P., P. Minnis, Y. H. Yi, et al., 2007: Summer dust aerosols detected from CALIPSO over the Tibetan Plateau. *Geophys. Res. Lett.*, **34**, doi: 10.1029/2007GL029938.

Huang, J. P., Z. W. Huang, J. R. Bi, et al., 2008a: Micro-pulse Lidar measurements of aerosol vertical structure over the Loess Plateau. *Atmos. Ocean. Sci. Lett.*, **1**, 8–11.

Huang, J. P., P. Minnis, B. Chen, et al., 2008b: Long-range transport and vertical structure of Asian dust from CALIPSO and surface measurements during PACDEX. *J. Geophys. Res.*, **113**, D23212, doi: 10.1029/2008JD010620.

Huang, J., Q. Fu, J. Su, et al., 2009: Taklimakan dust aerosol radiative heating derived from CALIPSO observations using the Fu–Liou radiation model with CERES constraints. *Atmos. Chem. Phys.*, **9**, 4011–4021, doi: 10.5194/acp-9-4011-2009.

Huang, J., P. Minnis, H. Yan, et al., 2010: Dust aerosol effect on semi-arid climate over Northwest China detected from A-Train satellite measurements. *Atmos. Chem. Phys.*, **10**, 6863–6872, doi: 10.5194/acp-10-6863-2010.

Huang, J. P., Q. Fu, W. Zhang, et al., 2011: Dust and black carbon in seasonal snow across northern China. *Bull. Amer. Meteor. Soc.*, **92**, 175–181, doi: 10.1175/2010BAMS3064.1.

Huang, J., X. Guan, and F. Ji, 2012: Enhanced cold-season warming in semi-arid regions. *Atmos. Chem. Phys.*, **12**, 5391–5398, doi: 10.5194/acpd-12-4627-2012.

Huang, X. X., T. J. Wang, F. Jiang, et al., 2013: Studies on a severe dust storm in East Asia and its impact on the air quality of Nanjing, China. *Aerosol and Air Quality Research*, **13**, 179–193, doi: 10.4209/aaqr.2012.05.0108.

Huang, J. P., T. H. Wang, W. C. Wang, et al., 2014: Climate effects of dust aerosols over East Asian arid and semi-arid regions. *J. Geophys. Res.*, **119**, 11398–11416, doi: 10.1002/2014JD021796.

Huang, J. P., J. J. Liu, B. Chen, et al., 2015: Detection of anthropogenic dust using CALIPSO lidar measurements. *Atmos. Chem. Phys.*, **15**, 11653–11655, doi: 10.5194/acp-15-11653-2015.

Huang, J. P., H. P. Yu, X. D. Guan, et al., 2016: Accelerated dryland expansion under climate change. *Nature Climate Change*, **6**, 166–171, doi: 10.1038/NCLIMATE2837.

Huneeus, N., M. Schulz, Y. Balkanski, et al., 2011: Global dust model intercomparison in AeroCom phase I. *Atmos. Chem. Phys.*, **11**, 7781–7816, doi: 10.5194/acp-11-7781-2011.

In, H.-J., and S.-U. Park, 2003: The soil particle size dependent emission parameterization for an Asian dust (Yellow Sand) observed in Korea in April 2002. *Atmos. Environ.*, **37**, 4625–4636, doi: 10.1016/j.atmosenv.2003.07.009.

Jia, X., W. C. Wang, Y. H. Chen, et al., 2010: Influence of dust aerosols on cloud radiative forcing over northern China. *China Environ. Sci*, **30**, 1009–1014. (in Chinese)

Jia, R., Y. Z. Liu, B. Chen, et al., 2015: Source and transportation of summer dust over the Tibetan Plateau. *Atmos. Environ.*, **123**, 210–219, doi: 10.1016/j.atmosenv.2015.10.038.

Joussaume, S, 1990: Three-dimensional simulations of the atmospheric cycle of desert dust particles using a general circulation model. *J. Geophys. Res.*, **95**, 1909–1941, doi: 10.1029/JD095iD02p01909.

Kameda, E. Azumi, A. Fukushima, et al., 2016: Mineral dust aerosols promote the formation of toxic nitropolycyclic aromatic compounds. *Scientific Report*, **6**, 24427, doi: 10.1038/srep24427.

Kang, J.-H., T.-C. Liu, J. Keller, et al., 2013: Asian dust storm events are associated with an acute increase in stroke hospitalisation. *Journal of Epidemiology and Community Health*, **67**, 125–131, doi: 10.1136/jech-2011-200794.

Kang, L., J. P. Huang, S. Y. Chen, et al., 2016: Long-term trends of dust events over Tibetan Plateau during 1961–2010. *Atmos. Environ.*, **125**, 188–198, doi: 10.1016/j.atmosenv.2015.10.085.

Kim, J., S.-C. Yoon, S.-W. Kim, et al., 2006: Chemical apportionment of shortwave direct aerosol radiative forcing at the Gosan super-site, Korea during ACE-Asia. *Atmos. Environ.*, **40**, 6718–6729, doi: 10.1016/j.atmosenv.2006.06.007.

Kim, N. K., Y. P.. Kim, and C.-H. Kang, 2011: Long-term trend of aerosol composition and direct radiative forcing due to aerosols over Gosan: TSP, $PM_{10}$, and $PM_{2.5}$ data between 1992 and 2008. *Atmos. Environ.*, **45**, 6107–6115, doi: 10.1016/j.atmosenv.2011.08.051.

Klose, M., and Y. P. Shao, 2012: Stochastic parameterization of dust emission and application to convective atmospheric conditions. *Atmos. Chem. Phys.*, **12**, 7309–7320, doi: 10.5194/acp-12-7309-2012.

Klose, M., and Y. P. Shao, 2013: Large-eddy simulation of turbulent dust emission. *Aeolian Research*, **8**, 49–58, doi: 10.1016/j.aerolia.2012.10.010.

Klose, M., Y. P. Shao, X. L. Li, et al., 2014: Further development of a parameterization for convective turbulent dust emission and evaluation based on field observations. *J. Geophys. Res.*, **119**, 10441–10457, doi: 10.1002/2014JD021688.

Kok, J. F., 2011: Does the size distribution of mineral dust aerosols depend on the wind speed at emission? *Atmos. Chem. Phys.*, **11**, 10149–10156, doi: 10.5194/acp-11-10149-2011.

Kuchiki, K., T. Aoki, M. Niwano, et al., 2015: Elemental carbon, organic carbon, and dust concentrations in snow measured with thermal optical and gravimetric methods: Variations during the 2007–2013 winters at Sapporo, Japan. *J. Geophys. Res.*, **120**, 868–882, doi: 10.1002/2014JA020661.

Lau, K. M., M. K. Kim, and K. M. Kim, 2006: Asian summer monsoon anomalies induced by aerosol direct forcing: The role of the Tibetan Plateau. *Climate Dyn.*, **26**, 855–864, doi: 10.1007/s00382-006-0114-z.

Lau, K.-M., S. C. Tsay, C. Hsu, et al., 2008: The joint aerosol–monsoon experiment: A new challenge for monsoon climate research. *Bull. Amer. Meteor. Soc.*, **89**, 369–389, doi: 10.1175/BAMS-89-3-369.

Lau, K. M., M. K. Kim, K.-M. Kim, et al., 2010: Enhanced surface warming and accelerated snow melt in the Himalayas and Tibetan Plateau induced by absorbing aerosols. *Environ. Res. Lett.*, **5**, doi: 10.1088/1748-9326/5/2/025204.

Li, J. W., Z .W. Han, and R. J. Zhang, 2011: Model study of atmospheric particulates during dust storm period in March 2010 over East Asia. *Atmos. Environ.*, **45**, 3954–3964, doi: 10.1016/j.atmosenv.2011.04.068.

Li, J., Z. Wang, G. Zhuang, et al., 2012: Mixing of Asian mineral dust with anthropogenic pollutants over East Asia: A model case study of a super-dust in March 2010. *Atmos. Chem. Phys.*, **12**, 7591–7607, doi: 10.5194/acp-12-7591-2012.

Liao, H., and J. H. Seinfeld, 1998: Radiative forcing by mineral dust aerosols: Sensitivity to key variables. *J. Geophys. Res.*, **103**, 31637–31645, doi: 10.1029/1998JD200036.

Liao, H., Y. Zhang, W.-T. Chen, et al., 2009: Effect of chemistry–aerosol–climate coupling on predictions of future climate and future levels of tropospheric ozone and aerosols. *J. Geophys. Res.*, **114**, D10306, doi: 10.1029/2008JD010984.

Liu, M., D. L. Westphal, S. G. Wang, et al., 2003: A high-resolution numerical study of the Asian dust storms of April 2001. *J. Geophys. Res.*, **108**, 8653, doi: 10.1029/2002JD003178.

Liu, Z. Y., D. Liu, J. P. Huang, et al., 2008: Airborne dust distributions over the Tibetan Plateau and surrounding areas derived from the first year of CALIPSO lidar observations. *Atmos. Chem. Phys.*, **8**, 5045–5060, doi: 10.5194/acp-8-5045-2008.

Liu, Y., D. X. Yang, W. Z. Chen, et al., 2010: Measurements of Asian dust optical properties over the Yellow Sea of China by shipboard and ground-based photometers, along with satellite remote sensing: A case study of the passage of a frontal system during April 2006. *J. Geophys. Res.*, **115**, doi: 10.1029/2009JD012684.

Liu, Y., J. Huang, G. Shi, et al., 2011: Aerosol optical properties and radiative effect determined from sky-radiometer over Loess Plateau of Northwest China. *Atmos. Chem. Phys.*, **11**, 11455–11463, doi: 10.5194/acp-11-11455-2011.

Liu, Y. Z., G. Y. Shi, and Y. K. Xie, 2013: Impact of dust aerosol on glacial–interglacial climate. *Adv. Atmos. Sci.*, **30**, 1725–1731, doi: 10.1007/s00376-013-2289-7.

Liu, Y. Z., R. Jia, T. Dai, et al., 2014: A review of aerosol optical properties and radiative effects. *J. Meteor. Res.*, **28**, 1003–1028, doi: 10.1007/s13351-014-4045-z.

Liu, Y., Y. Sato, R. Jia, et al., 2015: Modeling study on the transport of summer dust and anthropogenic aerosols over the Tibetan Plateau. *Atmos. Chem. Phys.*, **15**, 12581–12594, doi: 10.5194/acp-15-12581-2015.

Lu, H., and Y. P. Shao, 1999: A new model for dust emission by saltation bombardment. *J. Geophys. Res.*, **104**, 16827–16842, doi: 10.1029/1999JD900169.

Ma, J. H., H. Zhang, Y. F. Zheng, et al., 2007: The optical depth global distribution of dust aerosol and its possible reason analysis. *Climatic Environ. Res.*, **12**,156–164. (in Chinese)

Mahowald, N., K. Kohfeld, M. Hansson, et al., 1999: Dust sources and deposition during the last glacial maximum and current climate: A comparison of model results with paleodata from ice cores and marine sediments. *J. Geophys. Res.*, **104**, 15895–15916, doi: 10.1029/1999JD900084.

Marticorena, B., and G. Bergametti, 1995: Modeling the atmospheric dust cycle: 1. Design of a soil-derived dust emission scheme. *J. Geophys. Res.*, **100**, 16415–16430, doi: 10.1029/95JD00690.

Marticorena, B., G. Bergametti, B. Aumont, et al., 1997: Modeling the atmospheric dust cycle: 2. Simulation of Saharan dust sources. *J. Geophys. Res.*, **102**, 4387–4404, doi: 10.1029/96JD02964.

Mikami, M., G. Y. Shi, I. Uno, et al., 2006: Aeolian dust experiment on climate impact: An overview of Japan–China joint project ADEC. *Global and Planetary Change*, **52**, 142–172, doi: 10.1016/j.gloplacha.2006.03.001.

Ming, J., H. Cachier, C. Xiao, et al., 2008: Black carbon record based on a shallow Himalayan ice core and its climatic implications. *Atmos. Chem. Phys.*, **8**, 1343–1352, doi: 10.5194/acp-8-1343-2008.

Painter, T. H., A. P. Barrett, C. C. Landry, et al., 2007: Impact of disturbed desert soils on duration of mountain snow cover. *Geophys. Res. Lett.*, **34**, L12502, doi: 10.1029/2007GL030284.

Park, S.-U., and J. I. Jeong, 2008: Direct radiative forcing due to aerosols in Asia during March 2002. *Sci. Total Environ.*, **407**, 394–404, doi: 10.1016/j.scitotenv.2008.07.041.

Perlwitz, J., I. Tegen, and R. L. Miller, 2001: Interactive soil dust aerosol model in the GISS GCM: 1. Sensitivity of the soil dust cycle to radiative properties of soil dust aerosols. *J. Geophys. Res.*, **106**, 18167–18192, doi: 10.1029/2000JD900668.

Qian, Y., C. B. Fu, and S. Y. Wang, 1999: Mineral dust and climate change. *Adv. Earth Sci.*, **14**, 391–394. (in Chinese)

Qian, Y., W. I. Gustafson Jr, L. R. Leung, et al., 2009: Effects of soot-induced snow albedo change on snowpack and hydrological cycle in western United States based on Weather Research and Forecasting chemistry and regional climate simulations. *J. Geophys. Res.*, **114**, D03108, doi: 10.1029/2008JD011039.

Qian, Y., T. J. Yasunari, S. Doherty, et al., 2015: Light-absorbing particles in snow and ice: Measurement and modeling of climatic and hydrological impact. *Adv. Atmos. Sci.*, **32**, 64–91, doi: 10.1007/s00376-014-0010-0.

Qu, B., J. Ming, S.-C. Kang, et al., 2014: The decreasing albedo of the Zhadang glacier on western Nyainqentanglha and the role of light-absorbing impurities. *Atmos. Chem. Phys.*, **14**, 11117–11128, doi: 10.5194/acpd-14-13109-2014.

Shao, Y. P., 2001: A model for mineral dust emission. *J. Geophys. Res.*, **106**, 20239–20254, doi: 10.1029/2001JD900171.

Shao, Y. P., 2004: Simplification of a dust emission scheme and comparison with data. *J. Geophys. Res.*, **109**, D10202, doi: 10.1029/2003JD004372.

Shao, Y. P., 2008: *Physics and Modeling of Wind Erosion*. 2nd ed. Springer, Netherlands, 452 pp.

Shao, Y. P., M. Raupach, and J. F. Leys, 1996: A model for predicting aeolian sand drift and dust entrainment on scales from paddock to region. *Australian Journal of Soil Research*, **34**, 309–342, doi: 10.1071/SR9960309.

Shao, Y. P., Y. Yan, J. J. Wang, et al., 2003: Northeast Asian dust storms: Real-time numerical prediction and validation. *J. Geophys. Res.*, **108**, 4691, doi: 10.1029/2003JD003667.

Shao, Y., and C. H. Dong, 2006: A review on East Asian dust storm climate, modeling and monitoring. *Global and Planetary Change*, **52**, 1–22, doi: 10.1016/j.gloplacha.2006.02.011.

Shao, Y. P., K.-H. Wyrwoll, A. Chappell, et al., 2011: Dust cycle: An emerging core theme in Earth system science. *Aeolian Research*, **2**, 181–204, doi: 10.1016/j.aeolia.2011.02.001.

Shi, G. Y., 1984: Effect of atmospheric overlapping bands and their treatment on the calculation of thermal radiation. *Adv. Atmos. Sci.*, **1**, 246–255, doi: 10.1007/BF02678137.

Shi, J.-H., H.-W. Gao, J. Zhang, et al., 2012: Examination of causative link between a spring bloom and dry/wet deposition of Asian dust in the Yellow Sea, China. *J. Geophys. Res.*, **117**, D17304, doi: 10.1029/2012jd017983.

Sokolik, I., and G. Golitsyn, 1993: Investigation of optical and radiative properties of atmospheric dust aerosols. *Atmos. Environ. Part A. General Topics*, **27**, 2509–2517, doi: 10.1016/0960-1686(93)90023-R.

Sokolik, I., and O. B. Toon, 1996: Direct radiative forcing by anthropogenic airborne mineral aerosols. *Nature*, **381**, 681–683, doi: 10.1038/381681a0.

Su, J., J. P. Huang, Q. Fu, et al., 2008: Estimation of Asian dust aerosol effect on cloud radiation forcing using Fu–Liou radiative model and CERES measurements. *Atmos. Chem. Phys.*, **8**, 2763–2771, doi: 10.5194/acp-8-2763-2008.

Sun, J. M., M. Y. Zhang, and T. Liu, 2001: Spatial and temporal characteristics of dust storms in China and its surrounding regions, 1960–1999: Relations to source area and climate. *J. Geophys. Res.*, **106**, 10325–10333, doi: 10.1029/2000JD900665.

Sun, H., Z. T. Pan, and X. D. Liu, 2012: Numerical simulation of spatial–temporal distribution of dust aerosol and its direct radiative effects on East Asian climate. *J. Geophys. Res.*, **117**, D13206, doi: 10.1029/2011JD017219.

Takemura, T., T. Nakajima, A. Higurashi, et al., 2003: Aerosol distributions and radiative forcing over the Asian Pacific region simulated by spectral radiation–transport model for aerosol species (SPRINTARS). *J. Geophys. Res.*, **108**, 8659, doi: 10.1029/2002JD003210.

Tanaka, T. Y., and M. Chiba, 2005: Global simulation of dust aerosol with a chemical transport model, MASINGAR. *J. Meteor. Soc. Japan*, **83A**, 255–278, doi: 10.2151/jmsj.83A.255.

Tegen, I., and I. Fung, 1994: Modeling of mineral dust in the atmosphere: Sources, transport, and optical thickness. *J. Geophys. Res.*, **99**, 22897–22914, doi: 10.1029/94JD01928.

Tegen, I., A. Lacis, and I. Fung, 1996: The influence on climate forcing of mineral aerosols from disturbed soils. *Nature*, **380**, 419–422, doi: 10.1038/380419a0.

Todd, M. C., D. B. Karam, C. Cavazos, et al., 2008: Quantifying uncertainty in estimates of mineral dust flux: An intercomparison of model performance over the Bodélé Depression, northern Chad. *J. Geophys. Res.*, **113**, D24107, doi: 10.1029/2008JD010476.

Toon, O. B., C. McKay, T. P. Ackerman, et al., 1989: Rapid calculation of radiative heating rates and photodissociation rates in inhomogeneous multiple scattering atmospheres. *J. Geophys. Res.*, **94**, 16287–16301, doi: 10.1029/JD094iD13p16287.

Uno, I., G. R. Carmichael, D. G. Streets, et al., 2003: Regional chemical weather forecasting system CFORS: Model descriptions and analysis of surface observations at Japanese island stations during the ACE-Asia experiment. *J. Geophys. Res.*, **108**, 8668, doi: 10.1029/2002JD002845.

Uno, I., Z. Wang, M. Chiba, et al., 2006: Dust model intercomparison (DMIP) study over Asia: Overview. *J. Geophys. Res.*, **111**, D12213, doi: 10.1029/2005JD006575.

Uno, I., K. Yumimoto, A. Shimizu, et al., 2008: 3D structure of Asian dust transport revealed by CALIPSO lidar and a 4DVAR dust model. *Geophys. Res. Lett.*, **35**, L06803, doi: 10.1029/2007GL032329.

Uno, I., K. Eguchi, K. Yumimoto, et al., 2009: Asian dust transported one full circuit around the globe. *Nature Geoscience*, **2**, 557–560, doi: 10.1038/NGEO583.

Uno, I., K. Eguchi, K. Yumimoto, et al., 2011: Large Asian dust layers continuously reached North America in April 2010. *Atmos. Chem. Phys.*, **11**, 7333–7341, doi: 10.5194/acp-11-7333-2011.

Wang, T. H., and Q. L. Min, 2008: Retrieving optical depths of optically thin and mixed-phase clouds from MFRSR measurements. *J. Geophys. Res.*, **113**, D19203, doi: 10.1029/2008JD009958.

Wang, T. H., and J. P. Huang, 2009: A method for estimating optical properties of dusty cloud. *Chinese Optics Letters*, **7**, 368–372, doi: 10.3788/COL20090705.0368.

Wang, Z. F., H. Ueda, and M. Y. Huang, 2000: A deflation module for use in modeling long-range transport of yellow sand over East Asia. *J. Geophys. Res.*, **105**, 26947–26959, doi: 10.1029/2000JD900370.

Wang, H., G. Y. Shi, A. Teruo, et al., 2004: Radiative forcing due to dust aerosol over East Asia–North Pacific region during spring 2001. *Chinese Sci. Bull.*, **49**, 2212–2219, doi: 10.1007/

BF03185790.

Wang, X. H., T. J. Wang, J. P. Tang, et al., 2005: Thermal diffusion characteristics of atmosphere-particle two phase flow in dust storm. *Heat Mass Transfer*, **41**, 306–314, doi: 10.1007/s00231-004-0533-5.

Wang, X., J. P. Huang, M. X. Ji, et al., 2008: Variability of East Asia dust events and their long-term trend. *Atmos. Environ.*, **42**, 3156–3165, doi: 10.1016/j.atmosenv.2007.07.046.

Wang, H., S. L. Gong, H. L. Zhang, et al., 2010: A new-generation sand and dust storm forecasting system GRAPES_CUACE/Dust: Model development, verification and numerical simulation. *Chinese Sci. Bull.*, **55**, 635–649, doi: 10.1007/s11434-009-0481-z.

Wang, W. C., J. P. Huang, P. Minnis, et al., 2010: Dusty cloud properties and radiative forcing over dust source and downwind regions derived from A-Train data during the Pacific Dust Experiment. *J. Geophys. Res.*, **115**, D00H35, doi: 10.1029/2010JD014109.

Wang, X., J. P. Huang, R. D. Zhang, et al., 2010: Surface measurements of aerosol properties over Northwest China during ARM China 2008 deployment. *J. Geophys. Res.*, **115**, D00K27, doi: 10.1029/2009JD013467.

Wang, Z. L., H. Zhang, X. S. Shen, et al., 2010: Modeling study of aerosol indirect effects on global climate with an AGCM. *Adv. Atmos. Sci.*, **27**, 1064–1077, doi: 10.1007/s00376-010-9120-5.

Wang, J., X. G. Xu, D. K., Henze, et al., 2012: Top-down estimate of dust emissions through integration of MODIS and MISR aerosol retrievals with the GEOS-Chem adjoint model. *Geophys. Res. Lett*, **39**, doi: 10.1029/2012GL051136.

Wang, S. H., N. C. Hsu, S. C. Tsay, et al., 2012: Can Asian dust trigger phytoplankton blooms in the oligotrophic northern South China Sea. *Geophys. Res. Lett.*, **39**, L05811, doi: 10.1029/2011GL050415.

Wang, X., S. J. Doherty, and J. P. Huang, 2013: Black carbon and other light-absorbing impurities in snow across northern China. *J. Geophys. Res.*, **118**, 1471–1492, doi: 10.1029/2012JD018291.

Wang, Z. L., H. Zhang, X. W. Jing, et al., 2013: Effect of non-spherical dust aerosol on its direct radiative forcing. *Atmos. Res.*, **120–121**, 112–126, doi: 10.1016/j.atmosres.2012.08.006.

Wang, Y., X. Liu, C. Hoose, et al., 2014: Different contact angle distributions for heterogeneous ice nucleation in the Community Atmospheric Model version 5. *Atmos. Chem. Phys.*, **14**, 10411–10430, doi: 10.5194/acp-14-10411-2014.

Wang, H., G. Y. Shi, B. Wang, et al., 2017: The impacts of dust aerosol from deserts of China on the radiative heating rate over desert sources and the North Pacific region. *Chinese J. Atmos. Sci*, **31**, 515–526. (in Chinese)

Warren, S. G., and W. J. Wiscombe, 1980: A model for the spectral albedo of snow. II: Snow containing atmospheric aerosols. *J. Atmos. Sci.*, **37**, 2734–2745, doi: 10.1175/1520-0469(1980)037<2734:AMFTSA>2.0.CO;2.

Wei, X. D., and H. Zhang, 2011: Analysis of optical properties of nonspherical dust aerosols. *Acta Optica Sinica*, **31**, 501002, doi: 10.3788/AOS201131.0501002. (in Chinese)

Westphal, D. L., O. B. Toon, and T. N. Carlson, 1988: A case study of mobilization and transport of Saharan dust. *J. Atmos. Sci.*, **45**, 2145–2175, doi: 10.1175/1520-0469(1988)045<2145:ACSOMA>2.0.CO;2.

Woodward, S., 2001: Modeling the atmospheric life cycle and radiative impact of mineral dust in the Hadley Centre climate model. *J. Geophys. Res.*, **106**, 18155–18166, doi: 10.1029/2000JD900795.

Wu, J., W. M. Jiang, W. G. Wang, et al., 2004: Simulation of distribution and radiative effects of dust aerosol in spring over China area. *J. Univ. Sci. Tech.* , **34**, 116–125. (in Chinese)

Wu, J., C. B. Fu, Z. W. Han, et al., 2010: Simulation of the direct effects of dust aerosol on climate in East Asia. *Particuology*, **8**, 301–307, doi: 10.1016/j.partic.2010.01.006.

Wu, L. T., H. Su, and J. H. Jiang, 2013: Regional simulation of aerosol impacts on precipitation during the East Asian summer monsoon. *J. Geophys. Res.*, **118**, 6454–6467, doi: 10.1002/jgrd.50527.

Xia, X. G., P. C. Wang, Y. S. Wang, et al., 2008: Aerosol optical depth over the Tibetan Plateau and its relation to aerosols over the Taklimakan Desert. *Geophys. Res. Lett.*, **35**, doi: 10.1029/2008GL034981.

Xu, B. Q., J. J. Cao, J. Hansen, et al., 2009: Black soot and the survival of Tibetan glaciers. *Proc. Natl. Acad. Sci. USA*, **106**, 22114–22118, doi: 10.1073/pnas.0910444106.

Xu, B. Q., J. J. Cao, D. R. Joswiak, et al., 2012: Post-depositional enrichment of black soot in snow-pack and accelerated melting of Tibetan glaciers. *Environ. Res. Lett.*, **7**, 014022, doi: 10.1088/1748-9326/7/1/014022.

Yan, H., Y. Qian, G. Lin, et al., 2014: Parametric sensitivity and calibration for the Kain–Fritsch convective parameterization scheme in the WRF model. *Climate Res.*, **59**, 135–147, doi: 10.3354/Cr01213.

Yang, B., Y. Qian, G. Lin, et al., 2012: Some issues in uncertainty quantification and parameter tuning: A case study of convective parameterization scheme in the WRF regional climate model. *Atmos. Chem. Phys.*, **12**, 2409–2427, doi: 10.5194/acp-12-2409-2012.

Yang, B., Y. Qian, G. Lin, et al., 2013: Uncertainty quantification and parameter tuning in the CAM5 Zhang–McFarlane convection scheme and impact of improved convection on the global circulation and climate. *J. Geophys. Res.*, **118**, 395–415, doi: 10.1029/2012jd018213.

Yang, B., Y. C. Zhang, Y. Qian, et al., 2015a: Calibration of a convective parameterization scheme in the WRF model and its impact on the simulation of East Asian summer monsoon precipitation. *Climate Dyn.*, **44**, 1661–1684, doi: 10.1007/s00382-014-2118-4.

Yang, B., Y. C. Zhang, Y. Qian, et al., 2015b: Parametric sensitivity analysis for the Asian summer monsoon precipitation simulation in the Beijing Climate Center AGCM, version 2.1. *J. Climate*, **28**, 5622–5644, doi: 10.1175/JCLI-D-14-00655.1.

Yumimoto, K., I. Uno, N. Sugimoto, et al., 2008: Adjoint inversion modeling of Asian dust emission using lidar observations. *Atmos. Chem. Phys.*, **8**, 2869–2884, doi: 10.5194/acp-8-2869-2008.

Yumimoto, K., K. Eguchi, I. Uno, et al., 2009: An elevated large-scale dust veil from the Taklimakan Desert: Intercontinental transport and three-dimensional structure as captured by CALIPSO and regional and global models. *Atmos. Chem. Phys.*, **9**, 8545–8558, doi: 10.5194/acp-9-8545-2009.

Yumimoto, K., K. Eguchi, I. Uno, et al., 2010: Summertime trans-

Pacific transport of Asian dust. *Geophys. Res. Lett.*, **37**, L18815, doi: 10.1029/2010GL043995.

Yin, Y., S. Wurzler, Z. Levin, et al., 2002: Interactions of mineral dust particles and clouds: Effects on precipitation and cloud optical properties. *J. Geophys. Res.*, **107**, AAC 19-1–AAC 19-14, doi: 10.1029/2001JD001544.

Yin, Y., and L. Chen, 2007: The effects of heating by transported dust layers on cloud and precipitation: A numerical study. *Atmos. Chem. Phys.*, **7**, 3497–3505, doi: 10.5194/acp-7-3497-2007.

Zender, C. S., and E. Y. Kwon, 2005: Regional contrasts in dust emission responses to climate. *J. Geophys. Res.*, **110**, D13201, doi: 10.1029/2004JD005501.

Zender, C. S., H. S. Bian, and D. Newman, 2003: Mineral dust entrainment and deposition (DEAD) model: Description and 1990s dust climatology. *J. Geophys. Res.*, **108**, doi: 10.1029/2002JD002775.

Zhang, X. Y., R. Arimoto, and Z. S. An, 1997: Dust emission from Chinese desert sources linked to variations in atmospheric circulation. *J. Geophys. Res.*, **102**, 28041–28047, doi: 10.1029/97JD02300.

Zhang, X. Y., S. L. Gong, T. L. Zhao, et al., 2003: Sources of Asian dust and role of climate change versus desertification in Asian dust emission. *Geophys. Res. Lett.*, **30**, 2272, doi: 10.1029/2003GL018206.

Zhang, H., Z. L. Wang, P. W. Guo, et al., 2009a: A modeling study of the effects of direct radiative forcing due to carbonaceous aerosol on the climate in East Asia. *Adv. Atmos. Sci.*, **26**, 57–66, doi: 10.1007/s00376-009-0057-5.

Zhang, H., J. H. Ma, and Y. F. Zheng, 2009b: A modeling study of global radiative forcing due to dust aerosol. *Acta Meteor. Sinica*, **69**, 510–521. (in Chinese)

Zhang, L., X. Cao, J. Bao, et al., 2010: A case study of dust aerosol radiative properties over Lanzhou, China. *Atmos. Chem. Phys.*, **10**, 4283–4293, doi: 10.5194/acp-10-4283-2010.

Zhang, H., J. H. Ma, and Y. F. Zheng, 2010: Modeling study of the global distribution of radiative forcing by dust aerosol. *Acta Meteor. Sinica*, **24**, 558–570.

Zhang, H., Z. L. Wang, Z. Z. Wang, et al., 2012: Simulation of direct radiative forcing of aerosols and their effects on East Asian climate using an interactive AGCM-Aerosol coupled system. *Climate Dyn.*, **38**, 1675–1693, doi: 10.1007/s00382-011-1131-0.

Zhao, T. L., S. L. Gong, X. Y. Zhang, et al., 2003: Modeled size-segregated wet and dry deposition budgets of soil dust aerosol during ACE-Asia 2001: Implications for trans-Pacific transport. *J. Geophys. Res.*, **108**, 8665, doi: 10.1029/2002JD003363.

Zhao, T. L., S. L. Gong, X. Y. Zhang, et al., 2006: A simulated climatology of Asian dust aerosol and its trans-Pacific transport. Part I: Mean climate and validation. *J. Climate.*, **19**, 88–103, doi: 10.1175/JCLI3605.1.

Zhao, W., H. N. Liu, and J. Wu, 2008: Radiative and climate effects of dust aerosol in springs over China. *J. Nanjing Univ. (Natural Sci.)*, **44**, 598–607. (in Chinese)

Zhao, C., X. Liu, L. R. Leung, et al., 2010: The spatial distribution of mineral dust and its shortwave radiative forcing over North Africa: Modeling sensitivities to dust emissions and aerosol size treatments. *Atmos. Chem. Phys.*, **10**, 8821–8838, doi: 10.5194/acp-10-8821-2010.

Zhao, C., X. Liu, L. R. Leung, et al., 2011: Radiative impact of mineral dust on monsoon precipitation variability over West Africa. *Atmos. Chem. Phys.*, **11**, 1879–1893, doi: 10.5194/acp-11-1879-2011.

Zhao, C., S. Chen, L. R. Leung, et al., 2013a: Uncertainty in modeling dust mass balance and radiative forcing from size parameterization. *Atmos. Chem. Phys.*, **13**, 10733–10753, doi: 10.5194/acp-13-10733-2013.

Zhao, C., X. Liu, Y. Qian, et al., 2013b: A sensitivity study of radiative fluxes at the top of atmosphere to cloud-microphysics and aerosol parameters in the community atmosphere model CAM5. *Atmos. Chem. Phys.*, **13**, 10969–10987, doi: 10.5194/acp-13-10969-2013.

Zhao, C., Z. Hu, Y. Qian, et al., 2014: Simulating black carbon and dust and their radiative forcing in seasonal snow: A case study over North China with field campaign measurements. *Atmos. Chem. Phys.*, **14**, 11475–11491, doi: 10.5194/acp-14-11475-2014.

Zhao, S. Y., X. F. Zhi, H. Zhang, et al., 2014: Primary assessment of the simulated climatic state using a coupled aerosol–climate model BCC_AGCM2.0.1_CAM. *Climatic Environ. Res.*, **19**, 265–277, doi: 10.3878/j.issn.1006-9585.2012.12015. (in Chinese)

Zhao, S. Y., H. Zhang, S. Feng, et al., 2015: Simulating direct effects of dust aerosol on arid and semi-arid regions using an aerosol–climate coupled system. *Int. J. Climatol.*, **35**, 1858–1866, doi: 10.1002/joc.4093.

Zhou, C. H., S. L. Gong, X. Y. Zhang, et al., 2008: Development and evaluation of an operational SDS forecasting system for East Asia: CUACE/dust. *Atmos. Chem. Phys.*, **8**, 787–798, doi: 10.5194/acp-8-787-2008.

Zou, L. W., Y. Qian, T. J. Zhou, et al., 2014: Parameter tuning and calibration of RegCM3 with MIT–Emanuel cumulus parameterization scheme over CORDEX East Asia domain. *J. Climate*, **27**, 7687–7701, doi: 10.1175/Jcli-D-14-00229.1.

Tech & Copy Editor: Lan YI
Language Editor: Colin SMITH